

Original Article

Induction of Indistinguishable Gene Expression Patterns in Rats by Vero Cell-Derived and Mouse Brain-Derived Japanese Encephalitis Vaccines

Haruka Momose[†], Jun-ichi Imai^{1†}, Isao Hamaguchi[†], Mika Kawamura^{1,2}, Takuo Mizukami, Seishiro Naito, Atsuko Masumi, Jun-ichi Maeyama, Kazuya Takizawa, Madoka Kuramitsu, Nobuo Nomura³, Shinya Watanabe¹, and Kazunari Yamaguchi*

Department of Safety Research on Blood and Biological Products, National Institute of Infectious Diseases, Tokyo 208-0011; ¹Department of Clinical Informatics, Tokyo Medical and Dental University, Tokyo 133-8519; ²Medicrome, Inc., Tokyo 151-0051; and ³Biological Information Research Center, National Institute of Advanced Industrial Science and Technology, Tokyo 135-0064, Japan

(Received July 8, 2009. Accepted November 12, 2009)

SUMMARY: Transcriptomics is an objective index that reflects the overall condition of cells or tissues, and transcriptome technology, such as DNA microarray analysis, is now being introduced for the quality control of medical products. In this study, we applied DNA microarray analysis to evaluate the character of Japanese encephalitis (JE) vaccines. When administered into rat peritoneum, Vero cell-derived and mouse brain-derived JE vaccines induced similar gene expression patterns in liver and brain. Body weights and blood biochemical findings were also similar after administration of the two vaccines. Our results suggest that the two JE vaccines are likely to have equivalent characteristics with regard to reactivity in rats.

INTRODUCTION

Japanese encephalitis (JE) is a seasonal and sporadic viral encephalitis in East Asia, caused by infection with the JE virus. The JE virus exists in a zoonotic cycle between mosquitoes and swine and/or water birds. Infectious mosquitoes transmit JE to humans, a dead-end host (1). The great majority of infections are not apparent; the incidence of JE is considered to be 1 case per 250 to 500 infections (2). Even if the disease becomes manifest, recovery from mild illness occurs in most cases. Severe infection can cause febrile headache syndrome, aseptic meningitis, or encephalitis after an incubation period of about 6 to 16 days (1). Once JE has developed, the fatality rate is relatively high, from 5 to 40%, depending on the outbreak. Permanent neurological or psychiatric sequelae are left in 45–70% of survivors (1–3). No specific treatments for JE are available; therefore, preventing virus infection with vaccination is the most effective form of defense.

The approved and widely used JE vaccine is manufactured from inactivated JE virus that has been propagated in mouse brain. This mouse brain-derived (MBD) vaccine is currently manufactured and used in Japan, Korea, Taiwan, Thailand, Vietnam, and India, and is licensed in the United States, Canada, Israel, Australia, and several other Asian countries. Vaccination has succeeded in the near elimination of JE in several countries.

The MBD JE vaccine is a very pure form; impurities are removed during the manufacturing process, especially brain-

derived matter (3). Thus the vaccine has been considered safe. However, adverse reactions, such as local reactions and mild systemic events, may occur in 10–30% of vaccinated subjects (3). Acute disseminated encephalomyelitis (ADEM) coinciding with the administration of MBD vaccines has been reported at frequencies of 1 to 2 out of 100,000 doses (2,3). In the wake of a severe case of ADEM, the recommendation for a program of routine childhood immunization against JE was suspended in Japan in 2005 (2,4). It is of great concern that non-immunized children are not given the JE vaccine in JE-infected areas of Japan.

To replace the current MBD vaccine, Vero cell-derived (VCD) vaccines have been developed (5–10). The cessation of using mouse brain for virus propagation is expected to reduce the incidence of severe adverse reactions, including ADEM, because myelin basic protein, which is abundant in the central nervous system, is a possible substrate that provokes ADEM (11). Further, a cell culture-based technique is advantageous for large-scale production of JE vaccine. The demand for JE vaccine is growing, because the distribution of the JE virus has expanded throughout Asia and towards the northern edge of Australia over the last decade (12,13), and these newly JE virus-infected countries will require JE vaccine.

Apart from these concerns about the JE vaccine, moving towards cell culture-based vaccines is a global trend in the field of virus vaccine development (14). Primary hamster kidney cells were the first cells to be accepted for the production of JE vaccine, and continue to be used in China and some other countries (3,15). Recently, vaccine production using primary cell culture systems has been replaced by production using continuous cell lines (CCLs), including the Vero cell line (14). The Vero cell line is the most widely accepted CCL by regulatory authorities and has been used for over 30 years for the production of polio and rabies virus vaccines (16,17). In addition, VCD vaccines for rotavirus, smallpox

*Corresponding author: Mailing address: Department of Safety Research on Blood and Biological Products, National Institute of Infectious Diseases, 4-7-1 Gakuen, Musashimurayama, Tokyo 208-0011, Japan. Tel: +81-42-561-0771, Fax: +81-42-565-3315, E-mail: kyama@nih.go.jp

[†]These authors contributed equally to the paper.

virus, and influenza virus have been developed (14,18). In the case of JE vaccines, one of the developed VCD vaccines has received recent approval in the United States and Europe. Another was licensed in Japan in February 2009.

A newly licensed VCD JE vaccine must be at least equivalent to the current high-quality MBD vaccine in effectiveness. In this study, we applied conventional animal tests to demonstrate the equivalence of the MBD JE vaccine and the VCD JE vaccine. Further, based on our previous studies demonstrating that DNA microarray analysis was able to assay the features of a vaccine with high sensitivity, comprehensive gene expression analysis was performed to characterize the physiological reactivity of both JE vaccines.

MATERIALS AND METHODS

Animals: Eight-week-old male Wistar rats, weighing 160–200 g, were obtained from SLC (Tokyo, Japan). Animals were housed in rooms maintained at $23 \pm 1^\circ\text{C}$, with $50 \pm 10\%$ relative humidity and 12-h light/dark cycles, for at least 1 week prior to the test challenge. All procedures used in this study complied with institutional policies of the Animal Care and Use Committee of the National Institute of Infectious Diseases.

Vaccines: The approved JE vaccine (MBD) is an inactivated, highly purified JE virus (Beijin-1 strain), propagated in mouse brain. The improved inactivated vaccine (VCD) is manufactured from the same strain in Vero cells. Both vaccines were generous gifts from Biken, The Research Foundation for Microbial Diseases of Osaka University, Japan. We administered 5 ml of MBD or VCD into rat peritoneum. Physiological saline (SA) was used as a control.

Weight check: The rat decreasing body weight test was performed according to the Minimum Requirements for Biological Products in Japan (19). After we injected 5 ml of samples into the peritoneum, animals were weighed daily. Five rats in each group were used.

Hematological test: Rats were treated with SA, MBD, or VCD, and blood samples were collected on days 1, 2, 3, and 4 after administration. Blood was immediately mixed with EDTA, and the number of erythrocytes, hematocrit level, hemoglobin value, number of leukocytes, and number of platelets (PLT) were determined using an automatic hemacytometer, the Celltac MEK-5254 (Nihon Kohden, Tokyo, Japan). Five rats in each group were used.

Serum test: Blood samples for the serum test were collected separately from the same rats used for the hematological test. After centrifugation at 3,000 rpm for 15 min, 10-fold diluted supernatants were used for subsequent tests. We measured the activity of glutamate oxaloacetate transaminase/aspartate aminotransferase (GOT/AST), glutamate pyruvate transaminase/alanine aminotransferase (GPT/ALT), alkaline phosphatase (ALP), amylase (AMYL), and creatine phosphokinase (CPK), and the quantity of blood urea nitrogen (BUN), creatinine (CRE), total cholesterol (TCHO), triglyceride (TG), glucose (GLU), and C-reactive protein (CRP) using a DRICHEM-3030 according to the manufacturer's instructions (Fujifilm, Japan). Five rats in each group were used.

RNA preparation: Rats were sacrificed to obtain the whole brain and the lateral left lobe of the liver. Tissues were immediately frozen in liquid nitrogen for storage. Thawed tissue was homogenized and mixed with Isogen reagent (NIPPON GENE, Tokyo, Japan). Total RNA was prepared from the lysate in accordance with the manufacturer's instruc-

tions. Poly(A)⁺ RNA was prepared from total RNA with a Poly(A) Purist Kit (Ambion, Austin, Tex., USA) according to the manufacturer's instructions.

Microarray preparation and expression profile acquisition: For microarray analysis, rats were treated with SA, MBD, or VCD (3 rats per treatment), and 2 tissue samples from each animal, brain and liver, were analyzed on days 1–4 post-treatment. A set of synthetic polynucleotides (80-mers) representing 11,468 rat transcripts and including most of the RefSeq genes deposited in the NCBI database (MicroDiagnostic, Tokyo, Japan) was arrayed on aminosilane-coated glass slides (Type I; Matsunami, Kishiwada, Japan) with a custom-made arrayer (20,21). Poly(A)⁺ RNA (1.5 μg) of each sample was labeled using SuperScript II (Invitrogen, Carlsbad, Calif., USA) with Cyanine 5-dUTP. A common reference RNA (MicroDiagnostic) was labeled with Cyanine 3-dUTP (PerkinElmer, Boston, Mass., USA). Labeling, hybridization, and washes of microarrays were performed with a Labeling & Hybridization Kit (MicroDiagnostic) according to the manufacturer's instructions. The common reference RNA was purchased as a single batch and was labeled with Cyanine-3 for a single microarray side by side with each sample labeled with Cyanine-5. Hybridization signals were measured using a GenePix 4000A scanner (Axon Instruments, Union City, Calif., USA) and then processed into primary expression ratios ([Cyanine 5-intensity obtained from each sample]/[Cyanine 3-intensity obtained from common reference RNA]), which are indicated as 'median of ratios' in GenePix Pro 3.0 software [Axon Instruments]). The GenePix Pro 3.0 software performed normalization for the median of ratios (primary expression ratios) by multiplying normalization factors calculated for each feature on a microarray.

Data analysis: Data processing and hierarchical cluster analysis were performed using Excel (Microsoft, Redmond, Wash., USA) and an MDI gene expression analysis software package (MicroDiagnostic). The primary expression ratios were converted into \log_2 values (\log_2 Cyanine-5 intensity/Cyanine-3 intensity) (designated log ratios) and compiled into a matrix (designated primary data matrix). To predict the most obvious differences obtained from cluster analysis of the primary data matrix, we extracted genes with \log_2 ratios over 1 or under -1 in at least 1 sample from the primary data matrix and subjected them to two-dimensional hierarchical cluster analysis for samples and genes.

To identify genes demonstrating significant changes in expression, we extracted genes by *t* test between SA- and MBD-, SA- and VCD-, or MBD- and VCD-treated samples ($P < 0.01$).

RESULTS

Vaccine-treated animals showed no weight loss: Vaccines for public use are all made according to Good Manufacturing Practice (GMP), and many tests must be done before releasing vaccines to assure their quality. Conventional animal tests including the decreasing body weight test are applied for the quality control of vaccines (19). To explore the effects of the JE vaccines in a conventional method, we first applied the decreasing body weight test to the MBD and VCD JE vaccines, as described in Minimum Requirements for Biological Products in Japan (19). For this test, 5 ml of the vaccine was injected into the rat peritoneum, and the weight of the treated rats was measured daily for 4 days. As shown in Fig. 1, VCD-treated rats (filled circles) did not show

any weight loss, and gained weight in a similar manner to that of the SA- and MBD-treated groups (open and gray squares, respectively). Further, no abnormalities were observed in the condition or behavior of the rats during the testing period. Severe toxicity of MBD and VCD was not detected from this test.

Hematological tests revealed no significant changes in vaccinated rats: To investigate the influence of JE vaccines on hematological parameters, we treated rats with SA, MBD, or VCD (5 rats per treatment) and collected blood samples on days 1, 2, 3, and 4 after administration. We counted erythrocytes, leukocytes, and PLT and measured hematocrit levels and hemoglobin values. At any time point, all characteristics examined were within normal ranges and showed no significant differences among SA-, MBD-, and VCD-treated groups (Fig. 2). These results indicated that neither MBD nor VCD exhibited hematotoxicity to the treated rats.

Normal levels were observed in serum tests in vaccine-treated rats: To evaluate the reactivity of JE vaccines on

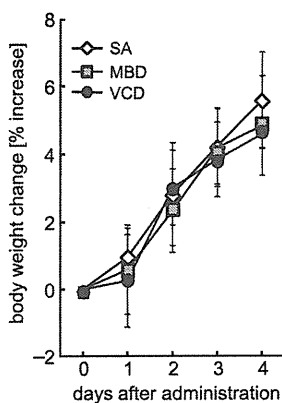


Fig. 1. Body weight analysis of the JE vaccine treated animals. The effects of mouse brain-derived (MBD) JE vaccine, Vero cell-derived (VCD) JE vaccine, and saline (SA) treatment were measured using decreasing body weight toxicity tests. All rats were weighed at days 0, 1, 2, 3, and 4. Changes in rat body weight were assessed as the percentage increase or decrease, and are indicated by the mean change \pm S.D.

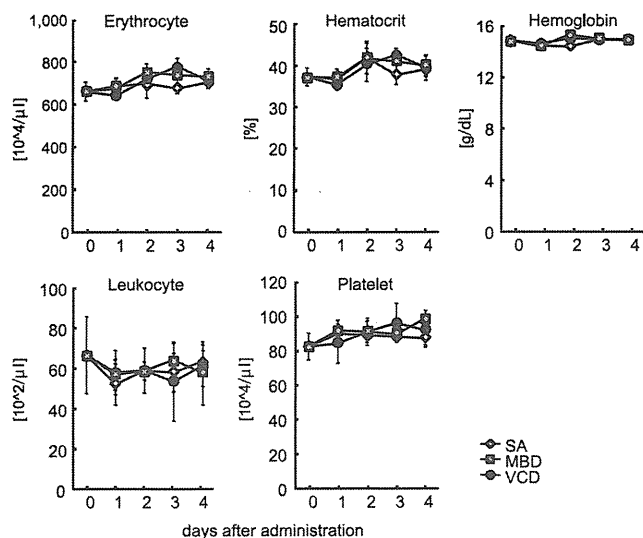


Fig. 2. Hematological tests for vaccinated rats. Blood obtained from individual rats was subjected to hematological tests. The tests were performed for 4 consecutive days after SA (open square), MBD (gray square), and VCD (filled circle) administration. Values are expressed as mean \pm S.D.

biological functions, we performed serum tests on vaccine-administered rats. On days 1, 2, 3, and 4 after administration of SA, MBD, or VCD, we collected blood from the same rats used for hematological tests, and isolated serum. Each serum sample was tested for liver function, renal function, muscle dysfunction, and metabolic abnormalities. No significant increase was observed in GOT/AST, GPT/ALT, ALP, or AMYL in any samples tested, indicating that no liver damage had occurred (Fig. 3 top panels). CRP values were all below detection limits (data not shown). Tests of renal (BUN and CRE) and muscle (CPK) function and of metabolism (TCHO, TG, and GLU) showed no differences among the vaccine-treated groups (Fig. 3 middle and bottom panels). These results suggested that SA, MBD, and VCD had similar biological reactivity in rats.

Microarray analysis of tissues from vaccine-treated rats: Although the animal tests described above have long been accepted for the quality control of biological reagents (22–24), the progress of molecular biotechnology presents the possibility to improve or renew the traditional tests. Among recent technologies, the high-throughput ‘omics’-based technologies have led the way to clarify immune responses to pathogens and responses of metabolic pathways, as well as to develop new vaccine candidates (25–27). Now, several efforts have been made to analyze the side effects of pharmaceuticals using one of the ‘omics’ technologies, transcriptomics (28,29). In this context, we performed DNA microarray analysis of the vaccinated rat tissues, liver and brain, and tried to determine the effects of MBD and VCD by analyzing gene expression patterns. The liver is thought to be one of the most appropriate organs to analyze biological alterations due to vaccination, because it is the major organ of metabolism. The brain was taken as another target tissue because a neurological effect can be one of the side effects of JE vaccination.

For the analysis, SA-, MBD-, and VCD-treated rats (3 rats per group) were sacrificed to obtain the liver and brain on days 1, 2, 3, and 4 post-administration. Thirty-six samples from each tissue type were obtained. Poly(A)⁺ RNA purified from the samples and a rat common reference RNA were labeled with Cyanine-5 and Cyanine-3, respectively, and hybridized to microarrays representing 11,468 transcripts. Hybridization signals were processed into expression ratios as \log_2 values (designated log ratios) and compiled into a matrix designated as the primary data matrix (see Materials and Methods).

To predict the most obvious differences obtained from the cluster analysis, we extracted genes with log ratios over 1 or under -1 in at least 1 sample in each group. Eventually, 2,386 genes for liver and 4,075 genes for brain were extracted and subjected to two-dimensional hierarchical cluster analysis for samples and genes (Fig. 4A). With hierarchical cluster analysis, genes were grouped according to expression patterns; thus samples having a similar gene expression pattern were clustered together, and samples having a distinct gene expression pattern formed a separate cluster (Fig. 4A) (30–32). If all test samples showed similar gene expression patterns, no clear clusters were formed. Thus, whether distinct clusters were formed was the criterion for the assessment of whether treatment with the 2 vaccines induced different gene expression patterns. Each column represents a sample. Each row represents a gene, and gene expression values are typically illustrated by a colored rectangle, red for up-regulation, blue for down-regulation, and yellow for no change. As shown, no

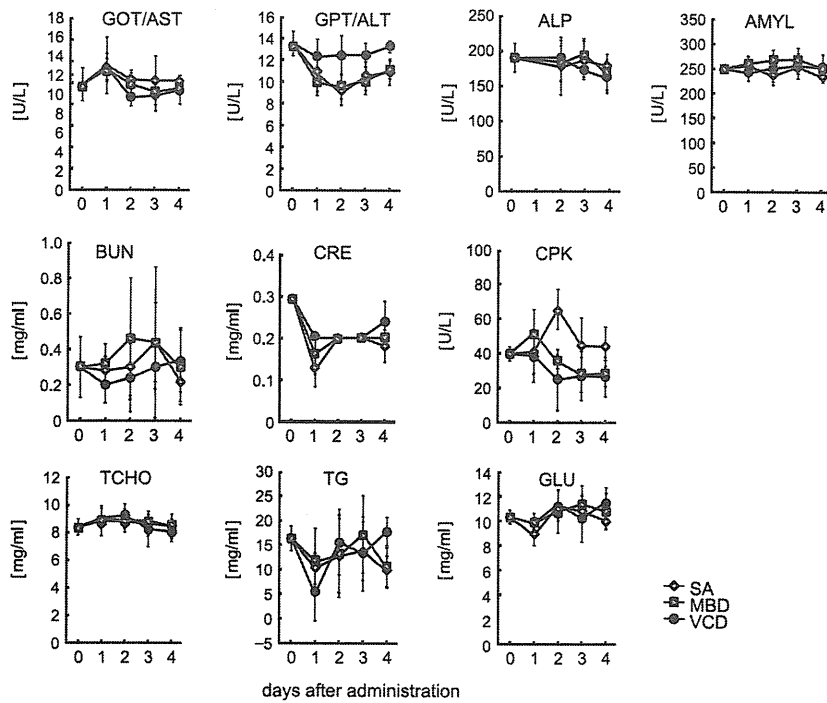


Fig. 3. Serum tests for vaccinated rats. Serum was separated from blood obtained from individual rats, and subjected to serum tests. The tests were performed for 4 consecutive days after SA (open square), MBD (gray square), and VCD (filled circle) administration. Values are expressed as mean \pm S.D.

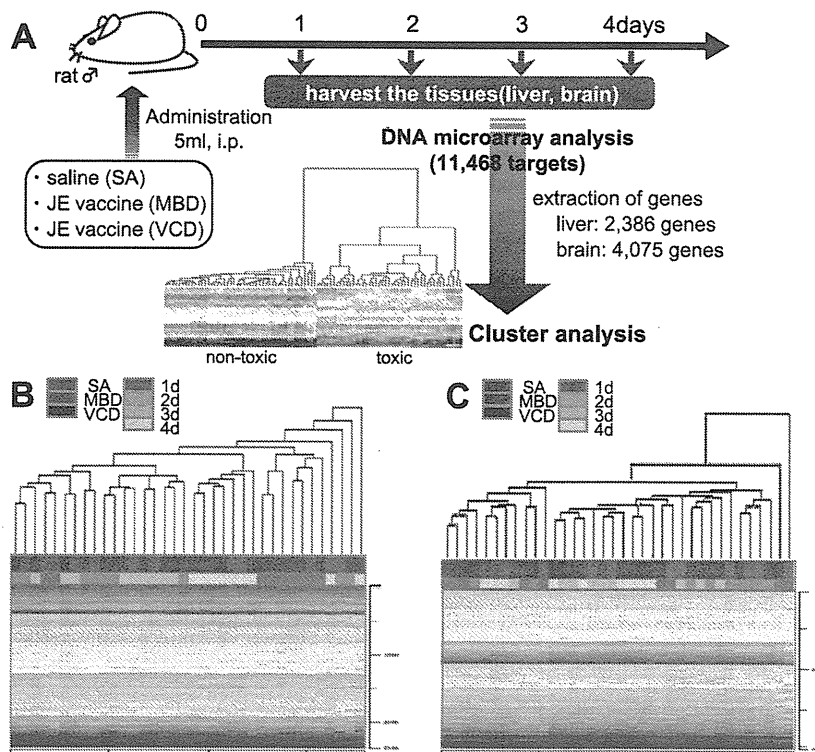


Fig. 4. Gene expression profiling and cluster analysis of vaccine-treated rat tissues. The procedure for gene expression analysis is outlined in A. For the cluster analysis, 2,386 genes for liver (B) and 4,075 genes for brain (C) were extracted from 11,468 targets and assembled in the order obtained from the results of the two-dimensional hierarchical cluster analysis. The results were drawn as a dendrogram based on the similarities of gene expression patterns of each sample. The y -axis of the dendrogram shown in (B) and (C) depicts the Euclid square distance as the dissimilarity coefficient, indicating the relationship between the samples. Red and blue indicate increases and decreases in the expression ratio, respectively.

clear clusters, corresponding to distinguishable gene expression patterns, were apparent, either in liver (Fig. 4B) or in brain (Fig. 4C). Gene expression patterns were very similar

in all vaccine-treated samples.

Further, we tried to identify specific genes whose expression levels were changed following JE vaccine treatment.

However, no genes could be selected from the comparison between MBD- and VCD-treated groups. MBD and VCD treatment could not be distinguished by gene expression analyses, indicating equivalent characteristics of MBD and VCD.

DISCUSSION

Comprehensive gene expression analysis is now an established approach to analyzing the effects of any manipulation on the whole transcriptome of living organisms. The genomic data associated with drug responses are expected to aid in the analysis of inter-individual variability and the tailoring of the administration of drugs to individuals to achieve maximal efficacy and minimum risk. The US Food and Drug Administration (FDA) now encourages voluntary genomic data submissions to the agency as part of new drug applications and biologics licensing applications (33). In this context, we have been trying to introduce DNA microarray analysis to the conventional quality control tests of the pertussis and influenza vaccines. The results of DNA microarray analysis correlated well with the results of conventional animal tests, and toxicity-related biomarkers were successfully extracted from the analysis (30–32). In the present study, we further applied this DNA microarray technology to analyze the biological reactivity of the JE vaccines (MBD and VCD). In liver and brain, the overall gene expression patterns were similar between MBD- and VCD-treated rats (Fig. 4), which was in accordance with the results obtained from the decreasing body weight test (Fig. 1) or the blood and serum tests (Figs. 2 and 3).

ADEM, an adverse reaction associated with JE vaccination, is thought to be a monophasic autoimmune disorder of the central nervous system, typically following a febrile infection or a vaccination (34). The precise mechanisms of ADEM have not been fully elucidated; however, recent studies suggested the involvement of inflammatory cytokines, such as tumor necrosis factor (TNF)- α and chemokines (35–37). Further, several genes associated with inflammation or immune responses, including *Irf7*, were up-regulated in JE virus-infected mouse brains (38,39). Therefore, inflammation above certain levels may be associated with adverse reactions to vaccines, that is, inflammation-related genes could be markers to detect contaminating toxicity that can cause adverse reactions. However, we found no significant changes in the expression levels of inflammatory genes between MBD- and VCD-treated rat tissues. We showed by using animal tests and comprehensive gene expression analysis that the two Japanese encephalitis vaccines, the existing MBD and the improved VCD vaccines, seemed to possess identical biological reactivity in rats.

To address concern about the reliability of the genomic data obtained from DNA microarray analysis, the FDA recently launched the MicroArray Quality Control (MAQC) project in anticipation of the regulatory submission of pharmacoinformatic and toxicoinformatic data in applications or supplements (33). The results of the MAQC project, showing interplatform reproducibility, were reported in 2006 (40–45). Subsequently, the follow-up MAQC-II project is progressing towards the development and the validation of genomic data in clinical applications. Similarly, in Japan, the Japan MicroArray Consortium (JMAC) for the standardization and the international harmonization of microarray platforms is ongoing and is coordinated with the FDA and the

European Medical Agency (EMA) (46). The efforts to achieve array platforms for the practical application of genomic data are being accelerated on a worldwide scale.

Although our experiments were limited with regard to the number of animals and vaccines examined, our DNA microarray technology was previously shown to be reproducible (30,32). The genomic data obtained in this study is, we believe, reliable. Recently, the VCD JE vaccine was licensed in Japan. It is desirable to accumulate gene expression profiles, especially data documenting the dynamics of inflammatory cytokines, in addition to generating animal testing data to enable a more reliable evaluation of the new JE vaccine.

ACKNOWLEDGMENTS

The authors thank Keiko Furuhashi and Momoka Tsuruhara for technical support.

This work was supported by Grants-in-Aid from the Ministry of Health, Labour and Welfare, Japan. The authors have no conflicting financial interests.

REFERENCES

1. Gubler, D.J., Kuno, G. and Markoff, L. (2007): Flaviviruses. p. 1185–1190. *In* D.M. Knipe, P.M. Howley, D.E. Griffin, et al. (ed.), *Fields Virology*. 5th ed. vol. I. Lippincott Williams & Wilkins, Philadelphia.
2. World Health Organization (2006): Japanese encephalitis vaccines. *Wkly. Epidemiol. Rec.*, 81, 331–340.
3. Halstead, S.B. and Jacobson, J. (2008): Japanese encephalitis vaccines. p. 311–352. *In* S.A. Plotkin, W.A. Orenstein, and P.A. Offit (ed.), *Vaccines*. 5th ed. Elsevier, New York.
4. Global Advisory Committee on Vaccine Safety, World Health Organization: Japanese encephalitis (JE) vaccines. Mouse brain-derived Japanese encephalitis (JE) vaccine. Online at <http://www.who.int/vaccine_safety/topics/japanese_encephalitis/mouse_brain_derived/en/>.
5. Hombach, J., Barrett, A.D., Cardosa, M.J., et al. (2005): Review on flavivirus vaccine development. Proceedings of a meeting jointly organised by the World Health Organization and the Thai Ministry of Public Health, 26–27 April 2004, Bangkok, Thailand. *Vaccine*, 23, 2689–2695.
6. Monath, T.P., Guirakhoo, F., Nichols, R., et al. (2003): Chimeric live, attenuated vaccine against Japanese encephalitis (ChimeriVax-JE): phase 2 clinical trials for safety and immunogenicity, effect of vaccine dose and schedule, and memory response to challenge with inactivated Japanese encephalitis antigen. *J. Infect. Dis.*, 188, 1213–1230.
7. Kuzuhara, S., Nakamura, H., Hayashida, K., et al. (2003): Non-clinical and phase I clinical trials of a Vero cell-derived inactivated Japanese encephalitis vaccine. *Vaccine*, 21, 4519–4526.
8. Abe, M., Shiosaki, K., Hammar, L., et al. (2006): Immunological equivalence between mouse brain-derived and Vero cell-derived Japanese encephalitis vaccines. *Virus Res.*, 121, 152–160.
9. Lyons, A., Kanesa-Thanan, N., Kuschner, R.A., et al. (2007): A Phase 2 study of a purified, inactivated virus vaccine to prevent Japanese encephalitis. *Vaccine*, 25, 3445–3453.
10. Tauber, E., Kollaritsch, H., Korinek, M., et al. (2007): Safety and immunogenicity of a Vero-cell-derived, inactivated Japanese encephalitis vaccine: a non-inferiority, phase III, randomised controlled trial. *Lancet*, 370, 1847–1853.
11. Pohl-Koppe, A., Burchett, S.K., Thiele, E.A., et al. (1998): Myelin basic protein reactive Th2 T cells are found in acute disseminated encephalomyelitis. *J. Neuroimmunol.*, 91, 19–27.
12. Williams, D.T., Wang, L.F., Daniels, P.W., et al. (2000): Molecular characterization of the first Australian isolate of Japanese encephalitis virus, the FU strain. *J. Gen. Virol.*, 81, 2471–2480.
13. Ritchie, S.A. and Rochester, W. (2001): Wind-blown mosquitoes and introduction of Japanese encephalitis into Australia. *Emerg. Infect. Dis.*, 7, 900–903.
14. Barrett, P.N., Mundt, W., Kistner, O., et al. (2009): Vero cell platform in vaccine production: moving towards cell culture-based viral vaccines. *Expert Rev. Vaccines*, 8, 607–618.
15. Petricciani, J. and Sheets, R. (2008): An overview of animal cell substrates for biological products. *Biologicals*, 36, 359–362.
16. Montagnon, B., Vincent-Falquet, J.C. and Fanget, B. (1983): Thousand litre scale microcarrier culture of Vero cells for killed polio virus vaccine. Promising results. *Dev. Biol. Stand.*, 55, 37–42.

17. Montagnon, B.J. (1989): Polio and rabies vaccines produced in continuous cell lines: a reality for Vero cell line. *Dev. Biol. Stand.*, 70, 27–47.
18. Monath, T.P., Caldwell, J.R., Mundt, W., et al. (2004): ACAM2000 clonal Vero cell culture vaccinia virus (New York City Board of Health strain)—a second-generation smallpox vaccine for biological defense. *Int. J. Infect. Dis.*, 8 Suppl 2, S31–44.
19. National Institute of Infectious Diseases, Japan (2006): Minimum Requirements for Biological Products. Online at <http://www.nih.go.jp/niid/MRBP/seibutsuki_english.pdf>.
20. Ito, E., Honma, R., Imai, J., et al. (2003): A tetraspanin-family protein, T-cell acute lymphoblastic leukemia-associated antigen 1, is induced by the Ewing's sarcoma-Wilms' tumor 1 fusion protein of desmoplastic small round-cell tumor. *Am. J. Pathol.*, 163, 2165–2172.
21. Kobayashi, S., Ito, E., Honma, R., et al. (2004): Dynamic regulation of gene expression by the Flt-1 kinase and Matrigel in endothelial tubulogenesis. *Genomics*, 84, 185–192.
22. Kurokawa, M. (1984): Toxicity and toxicity testing of pertussis vaccine. *Jpn. J. Med. Sci. Biol.*, 37, 41–81.
23. Horiuchi, Y., Takahashi, M., Konda, T., et al. (2001): Quality control of diphtheria tetanus acellular pertussis combined (DTaP) vaccines in Japan. *Jpn. J. Infect. Dis.*, 54, 167–180.
24. Mizukami, T., Masumi, A., Momose, H., et al. (2009): An improved abnormal toxicity test by using reference vaccine-specific body weight curves and histopathological data for monitoring vaccine quality and safety in Japan. *Biologicals*, 37, 8–17.
25. Grifantini, R., Bartolini, E., Muzzi, A., et al. (2002): Previously unrecognized vaccine candidates against group B meningococcus identified by DNA microarrays. *Nat. Biotechnol.*, 20, 914–921.
26. Yang, H.L., Zhu, Y.Z., Qin, J.H., et al. (2006): In silico and microarray-based genomic approaches to identifying potential vaccine candidates against *Leptospira interrogans*. *BMC Genomics*, 7, 293.
27. Shin, J., Wood, D., Robertson, J., et al. (2007): WHO informal consultation on the application of molecular methods to assure the quality, safety and efficacy of vaccines, Geneva, Switzerland, 7–8 April 2005. *Biologicals*, 35, 63–71.
28. Hamadeh, H.K., Bushel, P.R., Jayadev, S., et al. (2002): Gene expression analysis reveals chemical-specific profiles. *Toxicol. Sci.*, 67, 219–231.
29. Ejiri, N., Katayama, K., Kiyosawa, N., et al. (2005): Microarray analysis on Phase II drug metabolizing enzymes expression in pregnant rats after treatment with pregnenolone-16 α -carbonitrile or phenobarbital. *Exp. Mol. Pathol.*, 79, 272–277.
30. Hamaguchi, I., Imai, J., Momose, H., et al. (2007): Two vaccine toxicity-related genes Agp and Hpx could prove useful for pertussis vaccine safety control. *Vaccine*, 25, 3355–3364.
31. Mizukami, T., Imai, J., Hamaguchi, I., et al. (2008): Application of DNA microarray technology to influenza A/Vietnam/1194/2004 (H5N1) vaccine safety evaluation. *Vaccine*, 26, 2270–2283.
32. Hamaguchi, I., Imai, J., Momose, H., et al. (2008): Application of quantitative gene expression analysis for pertussis vaccine safety control. *Vaccine*, 26, 4686–4696.
33. Frueh, F.W. (2006): Impact of microarray data quality on genomic data submissions to the FDA. *Nat. Biotechnol.*, 24, 1105–1107.
34. Menge, T., Hemmer, B., Nessler, S., et al. (2005): Acute disseminated encephalomyelitis: an update. *Arch. Neurol.*, 62, 1673–1680.
35. Ichiyama, T., Shoji, H., Kato, M., et al. (2002): Cerebrospinal fluid levels of cytokines and soluble tumour necrosis factor receptor in acute disseminated encephalomyelitis. *Eur. J. Pediatr.*, 161, 133–137.
36. Kadhim, H., De Prez, C., Gazagnes, M.D., et al. (2003): In situ cytokine immune responses in acute disseminated encephalomyelitis: insights into pathophysiological mechanisms. *Hum. Pathol.*, 34, 293–297.
37. Franciotta, D., Zardini, E., Ravaglia, S., et al. (2006): Cytokines and chemokines in cerebrospinal fluid and serum of adult patients with acute disseminated encephalomyelitis. *J. Neurol. Sci.*, 247, 202–207.
38. Saha, S., Sugumar, P., Bhandari, P., et al. (2006): Identification of Japanese encephalitis virus-inducible genes in mouse brain and characterization of GARG39/IFIT2 as a microtubule-associated protein. *J. Gen. Virol.*, 87, 3285–3289.
39. Saxena, V., Mathur, A., Krishnani, N., et al. (2008): An insufficient anti-inflammatory cytokine response in mouse brain is associated with increased tissue pathology and viral load during Japanese encephalitis virus infection. *Arch. Virol.*, 153, 283–292.
40. Canales, R.D., Luo, Y., Willey, J.C., et al. (2006): Evaluation of DNA microarray results with quantitative gene expression platforms. *Nat. Biotechnol.*, 24, 1115–1122.
41. Shippy, R., Fulmer-Smentek, S., Jensen, R.V., et al. (2006): Using RNA sample titrations to assess microarray platform performance and normalization techniques. *Nat. Biotechnol.*, 24, 1123–1131.
42. Tong, W., Lucas, A.B., Shippy, R., et al. (2006): Evaluation of external RNA controls for the assessment of microarray performance. *Nat. Biotechnol.*, 24, 1132–1139.
43. Patterson, T.A., Lobenhofer, E.K., Fulmer-Smentek, S.B., et al. (2006): Performance comparison of one-color and two-color platforms within the MicroArray Quality Control (MAQC) project. *Nat. Biotechnol.*, 24, 1140–1150.
44. Shi, L., Reid, L.H., Jones, W.D., et al. (2006): The MicroArray Quality Control (MAQC) project shows inter- and intraplatform reproducibility of gene expression measurements. *Nat. Biotechnol.*, 24, 1151–1161.
45. Guo, L., Lobenhofer, E.K., Wang, C., et al. (2006): Rat toxicogenomic study reveals analytical consistency across microarray platforms. *Nat. Biotechnol.*, 24, 1162–1169.
46. Imagawa, K., Ito, T. and Azuma, J. (2008): The present status and future perspectives on pharmacogenomics and toxicogenomics. *Jpn. J. Clin. Pharmacol. Ther.*, 39, 61–67 (in Japanese).

Review Article

A New Method for the Evaluation of Vaccine Safety Based on Comprehensive Gene Expression Analysis

Haruka Momose,¹ Takuo Mizukami,¹ Masaki Ochiai,²
Isao Hamaguchi,¹ and Kazunari Yamaguchi¹

¹ Department of Safety Research on Blood and Biological Products, National Institute of Infectious Diseases,
4-7-1 Gakuen, Musashimurayama, Tokyo 208-0011, Japan

² Division of Quality Assurance, National Institute of Infectious Diseases, 4-7-1 Gakuen, Musashimurayama, Tokyo 208-0011, Japan

Correspondence should be addressed to Kazunari Yamaguchi, kyama@nih.go.jp

Received 30 September 2009; Accepted 2 April 2010

Academic Editor: Yongqun Oliver He

Copyright © 2010 Haruka Momose et al. This is an open access article distributed under the Creative Commons Attribution License, which permits unrestricted use, distribution, and reproduction in any medium, provided the original work is properly cited.

For the past 50 years, quality control and safety tests have been used to evaluate vaccine safety. However, conventional animal safety tests need to be improved in several aspects. For example, the number of test animals used needs to be reduced and the test period shortened. It is, therefore, necessary to develop a new vaccine evaluation system. In this review, we show that gene expression patterns are well correlated to biological responses in vaccinated rats. Our findings and methods using experimental biology and genome science provide an important means of assessment for vaccine toxicity.

1. Introduction

Vaccination effectively enables the control of many infectious diseases. However, we cannot always avoid the problem of adverse reactions accompanied by vaccination. While most adverse reactions are mild and local, some vaccines have been associated with very rare but severe systemic reactions. Therefore, all vaccines for public use are made in compliance with Good Manufacturing Practices (GMP) to prevent safety problems. Furthermore, manufacturers must submit samples and results of their in-house tests for each vaccine batch to the national control authorities before vaccines are released into the market. Among many quality control tests, conventional animal safety tests are performed to detect vaccine toxicity because residual vaccine toxicity has the potential to cause adverse reactions. For example, the animal body weight change test is the most commonly used test to evaluate the toxicity of vaccines [1]. Although a good correlation of the body weight loss with a vaccine's toxicity has been shown [2, 3], a greater understanding of the molecular mechanisms involved in the reaction to a vaccine's toxicity is needed. We, therefore, attempted to measure

animals' responses to vaccines by determining changes in gene expression profiles.

Gene expression profiling is a unique way to characterize how cells or tissues are affected by abnormal conditions. The measurement of gene expression levels upon exposure to toxicants can be used to identify toxic products, and to provide information about the mechanism of toxicity [4]. DNA microarray technology has opened the way for the parallel detection and analysis of expression patterns of thousands of genes in a single experiment. Furthermore, the development of high-quality gene arrays has allowed DNA microarray technology to become a standard tool in molecular toxicology. Recently, the field of toxicogenomics has validated the concept of gene expression profiles as "signatures" of toxicant classes [5–7]. These signatures have effectively directed the analytical search for predictive toxicant biomarkers and they have contributed to the understanding of the dynamic responses of molecular mechanisms associated with toxic responses. In fact, many studies of gene-expression profiles have now been reported in the toxicology field. For example, Hamadeh et al. reported patterns of gene expression in liver tissue taken from rats exposed to different

chemicals [8]. DNA microarray assays have also been applied to the analysis of the side effects of medicines [9]. Recently, the United States Food and Drug Administration (FDA) and the European Medicines Agency (EMA) have, either individually or together, started to review submissions for the qualification of biomarkers for medical products for specific purposes proposed by industry [10]. The introduction of pharmacogenomics, or pharmacogenetics, to the evaluation of medicines is a global trend.

For a better understanding of the molecular toxicology regarding vaccines, DNA microarray analysis promises to be an ideal method, as has been the case for pharmaceuticals. The FDA now encourages the voluntary submission of genomic data to the FDA outside of the regular review process [11]. However, no studies similar to those described above for pharmaceuticals have yet been conducted in the field of vaccines. At the beginning of this review, we summarized the current efforts used for the control of vaccine safety using conventional animal tests. We then referred to our recent efforts using DNA microarray analysis to identify “genetic signatures” for the toxicants remaining in vaccines. Since pertussis and influenza vaccines are among the most commonly used vaccines, we tried to develop a system to evaluate the “genetic signatures” of the toxicity of these vaccines.

2. Current Vaccine Safety Test

2.1. Body Weight Change in Vaccinated Animals. To screen for general toxicity of vaccines, the body weight of vaccine-treated animals can be analyzed as the general safety test [12]. Five mL of the vaccine are injected into the peritoneum of guinea pigs weighing 300–400 g, and the weight loss experienced by the animals is analyzed at days 1, 2, 3, 4, and 7 after administration. None of the animals should show any abnormal signs; no statistically significant ($P = .01$) difference in weight loss should be observed between the treated animals and the control group on any observation day. This test has been applied to a wide variety of vaccines in a unified way, and plays an important role in ensuring the safety and consistency of vaccine batches [12]. For pertussis vaccine (inactivated whole cell formulation), the effects of vaccine treatment were also measured using test for toxicity to mouse weight gain, in addition to the general safety test. All mice were weighed on days 0, 1, 2, 3, 4, and 7 after vaccine administration. The criterion for judgment is that mean body weight 3 days after injection should be no less than that at the time of injection upon statistical analysis, and no mice showed any abnormal sign during the observation periods [12]. When the reference vaccine (RE: the inactivated whole cell pertussis vaccine) was administered, weight loss was observed on day 1 after administration (Figure 1(a)).

2.2. Leukocytosis-Promoting Toxicity in Vaccinated Animals. To detect the toxin present in pertussis vaccines, the number of peripheral leukocytes can also be analyzed. Pertussis vaccine is injected into the peritoneum of mice at a dose of 0.5 mL. Leukocytes present in peripheral blood

are then counted 3 days after injection [12]. The white blood cell (WBC) counts in peripheral blood of reference vaccine-treated mice reach approximately 2,500 cells/ μ L (Figure 1(b)). The standard criterion of safety for pertussis vaccine (inactivated whole cell formulation) is that the mean count of leukocytes in peripheral blood, 3 days after injection, should not exceed 10 times that before injection [12].

2.3. Leukopenic Toxicity Test in Vaccinated Animals. Quality control of influenza vaccines is performed using the general safety test and the leukopenic toxicity test (LTT), which is based on peripheral WBC counts in mice 12–18 hours after intraperitoneal injection of a vaccine. The criterion for judgment is that the leukopenic toxicity of the test sample relative to that of the toxicity reference sample should be no higher than the value corresponding to 80% of the leukocyte count of the control relative to that of the toxicity reference sample [12–14].

3. DNA Microarray-Based Safety Test

The currently used quality control and safety tests, such as the LTT and the general safety test, have been used to evaluate vaccine safety for over 50 years [3]. We are now developing a new quality control method for vaccines using DNA microarray analysis as a substitute for the conventional animal tests [15–17]. The principle of this method is to translate vaccine quality, immunogenicity, and reactogenicity, into gene expression profile data. This method is expected to be informative, rapid, and highly sensitive.

For DNA microarray analysis using vaccines, 8 week-old male rats, weighing 180–220 g, were intraperitoneally administered with 5 mL of vaccine or physiological saline (SA). Three to 6 rats were used for each group. Vaccinated rats were sacrificed to obtain whole lung, kidney, brain, and the lateral left lobe of the liver on day 1, 2, 3, and 4 postadministration (Figure 2). Tissues were immediately frozen in liquid nitrogen for storage. Thawed tissue was homogenized and poly(A)⁺ RNA was purified from the lysate. Cyanine 5-labeled poly(A)⁺ RNA was subjected to DNA microarray analysis. Blood was also collected, however, this could not be analyzed due to the low quality of purified RNA.

For DNA microarray analysis, a set of synthetic polynucleotides (80-mers) representing 11,468 rat transcripts and including most of the RefSeq genes deposited in the NCBI database (MicroDiagnostic, Tokyo, Japan) was arrayed on aminosilane-coated glass slides [18, 19]. Cyanine 5-labeled poly(A)⁺ RNA was competitively hybridized on the slide with cyanine 3-labeled common reference RNA. Hybridization signals were measured, processed into primary expression ratios ([Cyanine 5-intensity obtained from each sample]/[Cyanine 3-intensity obtained from common reference RNA]), and then normalized by multiplying normalization factors calculated for each microarray feature.

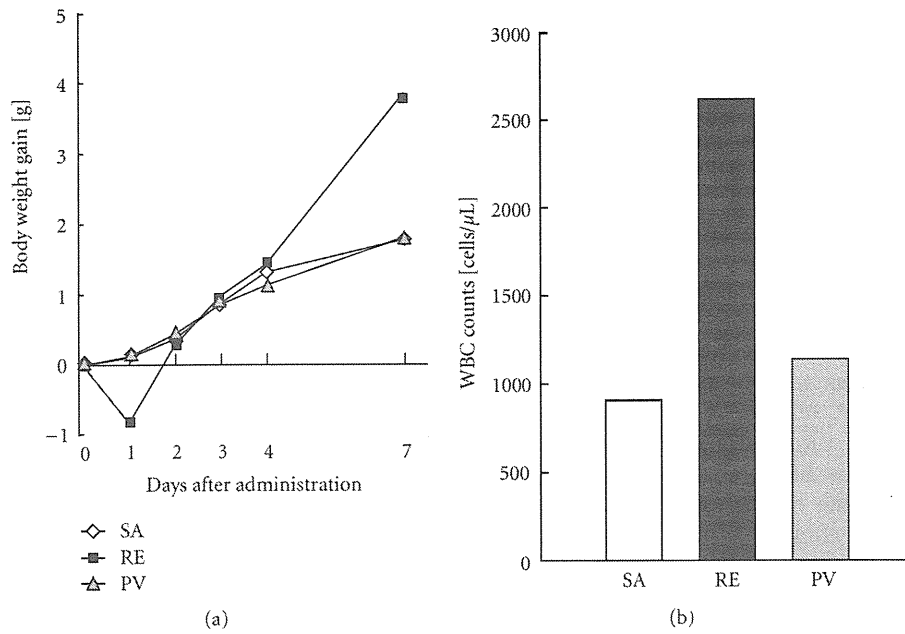


FIGURE 1: Safety control tests for pertussis vaccines. (a) Test for toxicity to mouse weight gain. Physiological saline (SA), an inactivated whole-cell pertussis vaccine (RE), or an acellular pertussis vaccine (PV)-administered mice were weighed on 0, 1, 2, 3, 4, and 7 days postadministration. Ten mice in each group were used, and the mean changes in body weight are indicated. (b) Leukocytosis promoting activity of various pertussis vaccines. White blood cell (WBC) counts in peripheral blood were measured 3 days after vaccine administration. Ten mice in each group were used and the mean WBC counts are indicated.

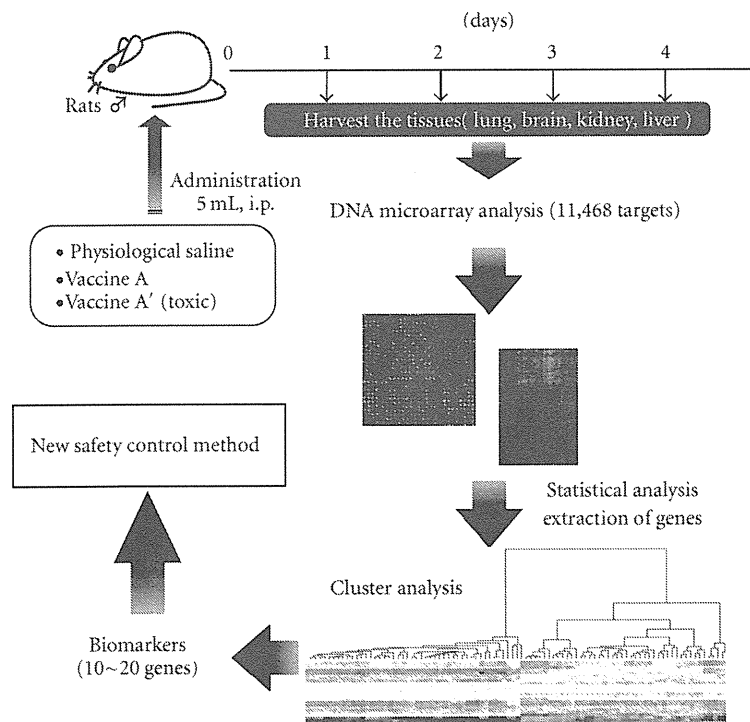


FIGURE 2: The gene expression analysis procedure. The detail of the procedure is described in the text.

For data processing and hierarchical cluster analysis, the primary expression ratios were converted into \log_2 ratios (\log_2 Cyanine-5 intensity/Cyanine-3 intensity). The genes with \log_2 ratios over 1 or under -1 in at least one sample were extracted from the primary data matrix, then subjected to two-dimensional hierarchical cluster analysis for samples and genes.

For the identification of biomarker genes for pertussis vaccines, we extracted differentially expressed genes from physiological saline and pertussis toxin-treated lung samples using the *t*-test ($P < .01$). Among the extracted genes, we further selected genes that exhibited mean average \log_2 ratio differences greater than 0.75 between the two sample groups [17]. For influenza vaccines, we extracted differentially expressed genes from physiological saline and inactivated whole-virion vaccine-treated lung samples using the *t*-test ($P < .005$) [16].

4. Pertussis Vaccines

Pertussis, or whooping cough, is an infectious respiratory disease caused by a Gram-negative bacillus, *Bordetella pertussis*. *Bordetella pertussis* possesses several pathogenic components, including pertussis toxin (PT) [20]. PT is known as a leukocytosis promoting factor, a major contributor to the pathogenesis of pertussis, and an antigen in immunity to pertussis [21]. At present, whole-cell pertussis vaccines and acellular pertussis vaccines containing inactivated PT are in commercial use [20].

Although pertussis vaccines are effective in the prevention of whooping cough, they have occasionally caused local reactions such as redness, swelling, and pain at the injection site. However, little is known about the overall responses to these vaccines. To address this problem, we applied DNA microarray analysis and quantification of specific genes to analyze the toxicants in pertussis vaccines [15, 17]. Three preparations, an acellular vaccine containing inactivated pertussis toxin (PV), an inactivated whole-cell vaccine (RE), and a purified pertussis toxin (PT) were prepared. RE is a reference vaccine for National Quality Control Tests of pertussis vaccines in Japan and is made from formaldehyde-inactivated *Bordetella pertussis* preparations. Physiological saline (SA) was used as a control. For comprehensive gene expression analysis, 5 mL of SA, PV, PT, and RE were each injected into 3 rats and the vaccinated tissues, lung, brain, kidney, and liver, were harvested at 1, 2, 3, and 4 days after vaccine administration. The experiments were performed twice and purified poly(A)⁺ RNA from a total of 384 samples was subjected to DNA microarray analysis.

Of the 4 organs tested, the lung expressed genes that were extracted by DNA microarray analysis were classified sharply into clusters depending on sample treatment. From the DNA microarray analysis of vaccinated rat lungs at day 1, 13 genes for which expression levels were dynamically changed in response to PT treatment were [17] (accession numbers were updated in Table 1). Interestingly, the DNA microarray-based gene expression data correlated well with the body weight change of vaccine-treated mice (Figure 1(a)) and rats [17]. The real-time PCR quantification results of

the expression levels of the 13 genes were comparable to the relative expression ratios from the DNA microarray analysis. Furthermore, cluster analysis using the 13 genes could distinguish SA- and PV-treated groups from PT- and RE-treated groups. These 13 genes are likely to be closely involved in the toxicity of pertussis vaccines. To quantify these genes in a convenient way, the QuantiGene Plex assay was applied. The QuantiGene Plex assay enabled the simultaneous analysis of the 13 genes. We evaluated the expression levels of the 13 genes in the lungs of rats vaccinated with various doses of RE. Nine genes, *S100A9*, *S100A8*, *IRF7*, *MX2*, *IFI27L*, *BEST5*, *MMP9*, *MMP8*, and *CYP2E1* (indicated in bold letters in Table 1) showed dose-dependent up- or down-regulation in response to the various doses of RE treatment. RE vaccine toxicity could be measured by the expression level in lung lysate of these 9 genes. The quantification of these 9 genes using the QuantiGene Plex assay is, we believe, a promising candidate for a new control test for pertussis vaccines.

5. Influenza Vaccines

Influenza virus triggers a highly contagious acute respiratory disease and has caused epidemics and global pandemics, partly because it possesses the capacity for gradual antigenic change in two surface antigens, hemagglutinin (HA) and neuraminidase (NA) [22]. To combat influenza, split vaccines consisting of subvirion preparations and whole-virus vaccines are manufactured using strains recommended annually by the WHO, based on the antigenic characteristics of HAs and NAs. Furthermore, the recent circulation of the highly pathogenic avian influenza A (H5N1) virus has raised concerns about the preparations for a coming influenza pandemic [23]. Many efforts are underway to develop vaccines against influenza A (H5N1).

To identify biomarkers for influenza vaccine toxicity, 3 vaccines were used: trivalent influenza HA vaccine (HA_v, a split vaccine), trivalent influenza vaccine (WP_v, an inactivated whole-virion vaccine), and prepandemic influenza vaccine (PD_v, inactivated whole-virion (A/H5N1) absorbed onto an aluminum salt). All were produced by Kaketsuken, The Chemo-Sero-Therapeutic Research Institute, Japan. Physiological saline (SA) was used as a control. For comprehensive gene expression analysis, SA, HA_v, WP_v, and PD_v were each injected into 5 rats, and the vaccinated tissues, lung, liver, brain, and peripheral blood, were harvested at 1, 2, 3, and 4 days after vaccine administration. Purified poly(A)⁺ RNA from a total of 320 samples was subjected to DNA microarray analysis [16]. Based on the analysis of pertussis vaccines, described above, the gene expression profiles from lung samples were subjected to two-dimensional hierarchical cluster analysis. PD_v- and WP_v-treated samples at day 1 formed an independent cluster from other samples, indicating distinct profiles in gene expression of these groups. As was the case with pertussis vaccines, we tried to identify several biomarkers from the analysis of lung gene expression. The analysis of lungs from vaccinated rats at day 1 resulted in the extraction of 76 genes, whose expression levels were statistically different between SA- and

TABLE 1: Biomarkers for pertussis vaccine toxicity.

Category	Accession no.	Symbol	Brief description
Inflammation	NM_053587	<i>S100A9</i>	A calcium binding protein that may be associated with acute inflammatory processes, coupled with S100a8
	NM_053822	<i>S100A8</i>	May play a role in inflammatory responses such as cell motility, coupled with S100a9
	NM_019323	<i>MCPT9</i>	A serine protease expressed in mast cells, but the precise function has not yet been determined
	NM_031530	<i>CCL2</i>	A ligand for CCR2 that acts as a chemoattractant of monocytes
IFN inducible, immune response	NM_001033691	<i>IRF7</i>	Unknown
	NM_134350	<i>MX2</i>	Involved in inhibiting vesicular stomatitis virus
	NM_203410	<i>IFI27</i>	Induced by steroid hormone, IFN, and LPS in endometrium at implantation, dendritic cells, and macrophages
	NM_001007694	<i>IFIT3</i>	May induced by IFN or virus infection
	Y07704	<i>BEST5</i>	Induced by IFN and involved in bone formation
Peptidoglycan metabolism	NM_031055	<i>MMP9</i>	Metalloproteinase involved in extracellular matrix remodeling, bone resorption, and immune responses
	NM_022221	<i>MMP8</i>	May play a role in appositional bone formation and regulation of the extracellular matrix
Xenobiotic metabolism	J02627	<i>CYP2E1</i>	Protects hepatocytes from stress-induced cell death
Others	NM_001106862	<i>NGP</i>	Unknown

TABLE 2: Biomarkers for influenza vaccine toxicity.

Category	Accession No.	Symbol	Brief description
IFN inducible gene	NM_172019	<i>IFI47</i>	Mouse homolog may be a guanine nucleotide-binding protein induced by IFN-gamma
	AF329825	<i>TRAFD1</i>	Putative TRAF-interacting zinc finger protein
	NM_019242	<i>IFRD1</i>	May be involved in proliferation of neuronal and glial precursors
IFN inducible, immune response	NM_001033691	<i>IRF7</i>	Unknown
	NM_134350	<i>MX2</i>	Involved in inhibiting vesicular stomatitis virus
Immune response	NM_172222	<i>C2</i>	Likely component of the classical pathway of the complement cascade
	NM_012708	<i>PSMB9</i>	Subunit of the proteasome complex, which may play a role in protein catabolism
	NM_032056	<i>TAP2</i>	Transports peptides into the ER lumen for binding with MHC class I molecules; plays a role in antigen processing and presentation
	NM_033098	<i>TAPBP</i>	Facilitates the binding of MHC class I molecules to the transporter associated with antigen processing (TAP) in MHC class I assembly
	NM_017264	<i>PSME1</i>	May play a role in proteasome activation
Chemokine and Cytokine function	AF065438	<i>LGALS3BP</i>	Displays differential expression in a fibroblast cell line transformed by human T-cell leukemia virus type 1 Tax protein
	NM_012977	<i>LGALS9</i>	A highly selective urate transporter/channel
	NM_053819	<i>TIMP1</i>	Acts as an inhibitor of metalloprotease activity; may play a role in vascular tissue remodeling
	NM_023981	<i>CSF1</i>	Plays a role in macrophage formation
	NM_145672	<i>CXCL9</i>	Chemokine which plays a role in the recruitment of mononuclear cells and in allograft rejection
	XM_223236	<i>CXCL11</i>	Mouse homolog is a chemokine and is involved in the immune response
Transcription activity	AJ302054	<i>ZBP1</i>	DNA binding protein; thought to bind Z-DNA, which is largely controlled by the amount of supercoiling

WPv-treated samples ($P < .005$) [16]. The cluster analysis using these 76 genes successfully distinguished WPv- and PDv-treated groups at day 1 from other groups, indicating the suitability of the 76 genes as biomarkers for influenza vaccines.

The extracted 76 genes were categorized according to function, such as interferon-inducible, chemokine and cytokine function, immune response, transcriptional activity, and so on. Among the 76 genes, 17 genes met the requirement for high expression levels and were chosen as representatives for each functional category (Table 2). Among the 17 genes, *IRF7* and *MX2* were also nominated for biomarkers of pertussis vaccine toxicity. Real-time PCR quantification results of the expression levels of the 17 genes were comparable to the relative expression ratios determined by DNA microarray analysis. We are now working to establish a rapid quantification system for these 17 biomarkers using the QuantiGene Plex assay.

6. Japanese Encephalitis Vaccines

Japanese encephalitis (JE) is a seasonal and sporadic encephalitis in East Asia caused by the JE virus. Vaccination is very important to prevent JE infection, because palliative care is the only treatment available for JE patients. Recently, a Vero cell-derived JE vaccine had been licensed in Japan as an alternative to the long-used mouse brain-derived JE vaccines. The newly developed Vero cell-derived vaccine should be at least equivalent to the mouse brain-derived vaccines, because the mouse brain-derived vaccines were considered generally safe and succeeded in the near elimination of JE in certain endemic regions. In this context, we performed DNA microarray analysis of tissues from rats administered with mouse brain-derived or Vero cell-derived JE vaccine and compared the gene expression profiles. As expected, the gene expression patterns in brain and liver were comparable between mouse brain-derived and Vero cell-derived vaccines, indicating that both vaccines possessed equivalent reactivity characteristics in rats [24].

7. Conclusions

Over recent decades, the safety control of vaccines has been assessed using several animal tests, including the body weight change test and white blood cell counts. However, conventional animal safety tests need to be improved in many aspects. For example, the number of test animals used needs to be reduced and the test period needs to be shortened. This requires the development of a new vaccine evaluation system. In this review, we showed that gene expression patterns were well correlated to the biological responsiveness of vaccinated animals. From the DNA microarray analysis of lungs from vaccinated rats, we identified 13 and 17 biomarkers to detect the toxicity of pertussis and influenza vaccines, respectively.

Furthermore, the QuantiGene Plex assay for gene expression analysis is being introduced. The QuantiGene Plex assay was revealed to be as accurate as real-time PCR and has

the great benefit of being able to evaluate all biomarkers simultaneously. Using the QuantiGene Plex assay, we could rapidly and sensitively detect the gene expression changes that accompany biological reactivity in vaccinated rats.

Thus, it may be concluded that DNA microarray technology is an informative, rapid, and highly sensitive method with which to evaluate vaccine quality. Our data suggest that this new method has the potential to shorten the time for safety tests and can reduce the number of animals used. In addition, our test may contribute to the development of urgently required vaccines. Further analyses are required to confirm that gene expression changes correlate with vaccine quality.

In this review, we referred to our recent efforts of exploring new safety control methods using gene expression pattern indexes, focusing on pertussis and influenza vaccines. In the future, for the evaluation of all kinds of vaccines, microarray analysis is expected to play an important role in the new safety control test, especially for checking toxin-reactive transcripts.

Acknowledgment

This work was supported by Grants-in-Aid from the Ministry of Health, Labour and Welfare, Japan.

References

- [1] Y. Horiuchi, M. Takahashi, T. Konda, et al., "Quality control of diphtheria tetanus acellular pertussis combined (DTaP) vaccines in Japan," *Japanese Journal of Infectious Diseases*, vol. 54, no. 5, pp. 167–180, 2001.
- [2] M. Kurokawa, "Toxicity and toxicity testing of pertussis vaccine," *Japanese Journal of Medical Science and Biology*, vol. 37, no. 2, pp. 41–81, 1984.
- [3] T. Mizukami, A. Masumi, H. Momose, et al., "An improved abnormal toxicity test by using reference vaccine-specific body weight curves and histopathological data for monitoring vaccine quality and safety in Japan," *Biologicals*, vol. 37, no. 1, pp. 8–17, 2009.
- [4] T. Lettieri, "Recent applications of DNA microarray technology to toxicology and ecotoxicology," *Environmental Health Perspectives*, vol. 114, no. 1, pp. 4–9, 2006.
- [5] E. K. Lobenhofer, P. R. Bushel, C. A. Afshari, and H. K. Hamadeh, "Progress in the application of DNA microarrays," *Environmental Health Perspectives*, vol. 109, no. 9, pp. 881–891, 2001.
- [6] W. Pennie, S. D. Pettit, and P. G. Lord, "Toxicogenomics in risk assessment: an overview of an HESI collaborative research program," *Environmental Health Perspectives*, vol. 112, no. 4, pp. 417–419, 2004.
- [7] A. H. Harrill and I. Rusyn, "Systems biology and functional genomics approaches for the identification of cellular responses to drug toxicity," *Expert Opinion on Drug Metabolism & Toxicology*, vol. 4, no. 11, pp. 1379–1389, 2008.
- [8] H. K. Hamadeh, P. R. Bushel, S. Jayadev, et al., "Gene expression analysis reveals chemical-specific profiles," *Toxicological Sciences*, vol. 67, no. 2, pp. 219–231, 2002.
- [9] N. Ejiri, K.-I. Katayama, N. Kiyosawa, Y. Baba, and K. Doi, "Microarray analysis on phase II drug metabolizing enzymes expression in pregnant rats after treatment with

- pregnenolone-16 α -carbonitrile or phenobarbital," *Experimental and Molecular Pathology*, vol. 79, no. 3, pp. 272–277, 2005.
- [10] European Medicines Agency Concept Paper, "Pharmacogenomics (PG) biomarker qualification: format and data standards," in *Proceedings of the International Conference on Harmonisation of Technical Requirements for Registration of Pharmaceuticals for Human Use*, June 2008, EMEA/CHMP/190395/2008, <http://www.emea.europa.eu/pdfs/human/pharmacogenetics/19039508en.pdf>.
- [11] F. W. Frueh, "Impact of microarray data quality on genomic data submissions to the FDA," *Nature Biotechnology*, vol. 24, no. 9, pp. 1105–1107, 2006.
- [12] *Minimum Requirements for Biological Products*, National Institute of Infectious Diseases, Tokyo, Japan, 2006, <http://www.nih.go.jp/niid/MRBP/files/seibutsuki.english.pdf>.
- [13] M. Kurokawa, S. Ishida, S. Asakawa, S. Iwasa, and N. Goto, "Toxicities of influenza vaccine: peripheral leukocytic response to live and inactivated influenza viruses in mice," *Japanese Journal of Medical Science and Biology*, vol. 28, no. 1, pp. 37–52, 1975.
- [14] F. Chino, "The views and policy of the Japanese control authorities on the three Rs," *Developments in Biological Standardization*, vol. 86, pp. 53–62, 1996.
- [15] I. Hamaguchi, J.-I. Imai, H. Momose, et al., "Two vaccine toxicity-related genes Agp and Hpx could prove useful for pertussis vaccine safety control," *Vaccine*, vol. 25, no. 17, pp. 3355–3364, 2007.
- [16] T. Mizukami, J.-I. Imai, I. Hamaguchi, et al., "Application of DNA microarray technology to influenza A/Vietnam/1194/2004 (H5N1) vaccine safety evaluation," *Vaccine*, vol. 26, no. 18, pp. 2270–2283, 2008.
- [17] I. Hamaguchi, J.-I. Imai, H. Momose, et al., "Application of quantitative gene expression analysis for pertussis vaccine safety control," *Vaccine*, vol. 26, no. 36, pp. 4686–4696, 2008.
- [18] E. Ito, R. Honma, J.-I. Imai, et al., "A tetraspanin-family protein, T-cell acute lymphoblastic leukemia-associated antigen 1, is induced by the Ewing's sarcoma-Wilms' tumor 1 fusion protein of desmoplastic small round-cell tumor," *American Journal of Pathology*, vol. 163, no. 6, pp. 2165–2172, 2003.
- [19] S. Kobayashi, E. Ito, R. Honma, et al., "Dynamic regulation of gene expression by the Flt-1 kinase and Matrigel in endothelial tubulogenesis," *Genomics*, vol. 84, no. 1, pp. 185–192, 2004.
- [20] K. M. Edwards and M. D. Decker, "Pertussis vaccines," in *Vaccines*, S. A. Plotkin, W. A. Orenstein, and P. A. Offit, Eds., pp. 467–517, Elsevier, New York, NY, USA, 5th edition, 2008.
- [21] H. Sato and Y. Sato, "Bordetella pertussis infection in mice: correlation of specific antibodies against two antigens, pertussis toxin, and filamentous hemagglutinin with mouse protectivity in an intracerebral or aerosol challenge system," *Infection and Immunity*, vol. 46, no. 2, pp. 415–421, 1984.
- [22] C. B. Bridges, J. M. Katz, R. A. Levandowski, and N. J. Cox, "Inactivated influenza vaccines," in *Vaccines*, S. A. Plotkin, W. A. Orenstein, and P. A. Offit, Eds., pp. 259–290, Elsevier, New York, NY, USA, 5th edition, 2008.
- [23] K. Ungchusak, P. Auewarakul, S. F. Dowell, et al., "Probable person-to-person transmission of avian influenza A (H5N1)," *The New England Journal of Medicine*, vol. 352, no. 4, pp. 333–340, 2005.
- [24] H. Momose, J.-I. Imai, I. Hamaguchi, et al., "Induction of indistinguishable gene expression patterns in rats by Vero cell-derived and mouse brain-derived Japanese encephalitis vaccines," *Japanese Journal of Infectious Diseases*, vol. 63, no. 1, pp. 25–30, 2010.

HIV-1 Nef impairs multiple T-cell functions in antigen-specific immune response in mice

Hideki Fujii^{1,2,*}, Manabu Ato^{2,*}, Yoshimasa Takahashi², Kaori Otake³, Shu-ichi Hashimoto⁴, Tomohiro Kaji⁵, Yasuko Tsunetsugu-Yokota², Mikako Fujita⁶, Akio Adachi⁷, Toshinori Nakayama⁸, Masaru Taniguchi⁹, Shigeo Koyasu¹ and Toshitada Takemori^{2,5}

¹Department of Microbiology and Immunology, Keio University School of Medicine, Tokyo 160-8582, Japan

²Department of Immunology, National Institute of Infectious Diseases, Tokyo 162-8640, Japan

³Gifu Social Insurance Hospital, Gifu 509-0206, Japan

⁴Chiome Bioscience Inc., Saitama 351-0104, Japan

⁵Laboratory for Immunological Memory, Riken Research Center for Allergy and Immunology, Kanagawa 230-0045, Japan

⁶Department of Bioorganic Medicinal Chemistry, Faculty of Medical and Pharmaceutical Sciences, Kumamoto University, Kumamoto 862-0973, Japan

⁷Department of Virology, Institute of Health Biosciences, The University of Tokushima Graduate School, Tokushima 770-8503, Japan

⁸Department of Immunology, Graduate School of Medicine, Chiba University, Chiba 260-8670, Japan

⁹Laboratory for Immune Regulation, Riken Research Center for Allergy and Immunology, Kanagawa 230-0045, Japan

*These authors contributed equally to this study.

Correspondence to: T. Takemori; E-mail: mttoshi@rcai.riken.jp

Received 10 February 2011, accepted 2 May 2011

Abstract

The viral protein Nef is a key element for the progression of HIV disease. Previous *in vitro* studies suggested that Nef expression in T-cell lines enhanced TCR signaling pathways upon stimulation with TCR cross-linking, leading to the proposal that Nef lowers the threshold of T-cell activation, thus increasing susceptibility to viral replication in immune response. Likewise, the *in vivo* effects of Nef transgenic mouse models supported T-cell hyperresponse by Nef. However, the interpretation is complicated by Nef expression early in the development of T cells in these animal models. Here, we analyzed the consequence of Nef expression in ovalbumin-specific/CD4⁺ peripheral T cells by using a novel mouse model and demonstrate that Nef inhibits antigen-specific T-cell proliferation and multiple functions required for immune response *in vivo*, which includes T-cell helper activity for the primary and memory B-cell response. However, Nef does not completely abrogate T-cell activity, as defined by low levels of cytokine production, which may afford the virus a replicative advantage. These results support a model, in which Nef expression does not cause T-cell hyperresponse in immune reaction, but instead reduces the T-cell activity, that may contribute to a low level of virus spread without viral cytopathic effects.

Keywords: AIDS, acquired immunity, humoral response

Introduction

The Nef protein of the primate lentiviruses HIV-1/2 and the simian immunodeficiency virus (SIV) is expressed from the earliest stage of viral gene expression (reviewed in ref. 1). Nef-defective viruses cause a slow progression of clinical disease with reduced viral loads in humans and rhesus macaques with HIV-1/2 and SIV infection, respectively, indicating that Nef plays a crucial role in viral pathogenesis in human and non-human primates (reviewed in ref. 1). Nef associates with host cell membranes through N-terminal myristoylation and functions as an adaptor bringing together a large number of proteins in host cells, mainly protein kinases and

components of endocytic trafficking machinery (reviewed in ref. 1; refs 2–7).

Nef reduces surface level receptors, including CD4, the primary receptor for HIV and SIV and MHC class I and class II complex, facilitating HIV immune evasion and thus increases viral pathogenesis (reviewed in ref. 1). Additionally, extensive *in vitro* studies, mostly carried out by using human T-cell lines, have suggested that Nef expression enhances TCR-mediated signaling pathways and transcriptional activation (reviewed in ref. 1; refs 2–5). Such alterations in signaling events may lower the TCR activation threshold in CD4⁺

T cells and help more responsive to T-cell activation signals, a process that could support higher virus production upon stimuli mediated via the TCR (reviewed in ref. 1; refs 2–5). Moreover, Nef may alter host cell death pathways to prevent apoptosis of infected cells, thereby fostering their longevity (reviewed in ref. 1). These observations have led to a model in which Nef reorganizes the host cell activity so as to optimize viral propagation and cell survival, thus facilitating immune evasion and participating in virus spread.

The consequence of Nef expression in primary cells has been examined by using Nef transgenic (Tg) mice, in which Nef was constitutively or transiently expressed under control of a T-cell-specific promoter–enhancer element (8, 9). In this model system, Nef promotes T-cell activation, however, interpretation of these findings is complicated by the fact that expression of Nef early in the development of T cells results in wholesale depletion of thymocytes and peripheral T cells. Moreover, it remains obscure whether the T-cell activation seen in Nef Tg mice is mediated by lymphopenia-induced mechanisms rather than by an intrinsic effect of Nef expression on T-cell activation and proliferation (9, 10).

In the present study, to examine the consequence of Nef expression in primary cells, we established a double transgenic mouse (dTg), which expresses human coxsackie/adenovirus receptor (CAR) (11) and an ovalbumin (OVA)-specific TCR that recognizes the OVA peptide on antigen-presenting cell (APC) with high affinity under MHC Class II I-A^d-restriction. This system allowed us to analyze the effect of Nef on antigen-specific peripheral T-cell function by transfer of the *nef* gene into peripheral T cells using an adenovirus vector. The present study demonstrates that Nef expression does not cause T-cell hyperresponse but instead impairs T-cell functions required for immune response.

Methods

Mice

BALB/c and CB17-scid mice were purchased from Shizuoka Laboratory Animal Center (Hamamatsu, Japan) and Clea Japan, Inc. (Tokyo, Japan), respectively. Tg mice expressing the CAR under the control of the Lck proximal promoter (CAR Tg mice) on the BALB/c background have been described previously (11). DO11.10 mice express a transgenic TCR with specificity for OVA peptide residues 323–339 (OVA_{323–339}) restricted by I-A^d on the BALB/c background (12). All mice used in this study were maintained under specific pathogen-free conditions and used at 6–12 weeks of age in accordance with the guidelines of the Institutional Animal Care and Use Committee, National Institute of Infectious Diseases.

Adenovirus vector

Recombinant adenovirus vectors were generated using the AdEasy Adenoviral Vector System (Stratagene) according to the manufacturer's instructions. In order to express the *nef* gene under the CAG promoter, the pShuttle vector was digested with *KpnI*, blunt-ended with T4 polymerase and then, the CAG promoter DNA was ligated (pShuttle-CAG). Next, an *XhoI*–*XbaI* fragment of pIRES2-EGFP (Invitrogen)

was inserted into the *XhoI*–*XbaI* site of pShuttle-CAG, which was designated as pShuttle-CAG-I2-EGFP. HIV-1 NL4-3 *nef* wild-type and a mutant (⁵⁷W⁵⁸L to ⁵⁷A⁵⁸A) were PCR amplified from pNL432 and pNL-n57/2A proviral DNA, respectively, using specific primers containing *EcoRI* sites at both ends and then subcloned into pBluscript KS⁺ (Stratagene). The *EcoRI* fragment containing wild-type or mutant *nef* was inserted into the *EcoRI* site of pShuttle-CAG-I2-EGFP. These shuttle vectors were linearized and co-transformed into *Escherichia coli* strain BJ5183-AD-1, which contains the pAdEasy vector, to induce homologous recombination (Supplementary Figure 1 is available at *International Immunology Online*). Recombinant adenoviral plasmids were selected and transfected into 293 cells to produce recombinant adenovirus particles. Recombinant adenovirus were purified by two rounds of Cesium chloride density gradient centrifugation as described previously (13). The concentrated virus was dialyzed against PBS containing 10% glycerol. The titer of the virus stock was determined by a plaque formation assay using 293 cells.

T-cell purification and recombinant adenovirus infection

For recombinant adenovirus infection, CD4⁺ T cells were enriched by negative selection on a MACS column (Miltenyi Biotec GmbH, Gladbach, Germany) as previously described (14). Briefly, cells were blocked with anti-FcγRII/III (2.4G2; BD PharMingen, San Diego, CA, USA) and incubated with biotinylated mAbs against B220(RA3-6B2), IgM(II/41), IgD(11-26), Gr1(RB6-8C5), CD11c(N418), CD49b(DX5), CD11b(M1/70) and CD8(53–6.7) (eBioscience, San Diego, CA, USA), followed by incubation with streptavidin-coated microbeads (Miltenyi Biotec GmbH). Purified CD4⁺ T cells (>95%) were infected with recombinant adenovirus vector at a multiplicity of infection of 10 (MOI 10) for 2 days in 24-well plates at a concentration of 2×10^6 per well in RPMI 1640 medium supplemented with 10% Fetal Bovine Serum (FBS), 5×10^5 M 2-mercaptoethanol, L-glutamine, antibiotics and IL-7 (20 ng ml⁻¹; PeproTech, London, UK) at 37°C in an atmosphere of 5% CO₂.

Proliferation assays and ELISA

Sorted CD4⁺ GFP⁺ T cells were cultured in microtiter wells at a concentration of 4×10^4 cells per well in the presence of OVA_{323–339} peptide and 5×10^5 irradiated T-depleted spleen cells. DNA synthesis of cultured cells in triplicate was estimated by the incorporation of [³H] thymidine (0.5 μCi) added 12 h prior to cell harvest. The level of IFN-γ and IL-2 in the culture supernatants was measured by a Ready-Set-Go! ELISA assay kit (eBioscience), according to the manufacturer's instruction. In some experiments, CD4⁺ GFP⁺ T cells (2×10^6) were cultured for 2–3 days in 96-well plates immobilized with anti-TCR mAb (5 μg ml⁻¹) and anti-CD28 mAb (1 μg ml⁻¹) (BD PharMingen).

Chemotaxis assay

Chemotaxis assays were performed in Transwell (Corning Coster, Corning, NY, USA) with polycarbonate filters (5 μm pore size) as described previously (15). Briefly, purified CD4⁺ GFP⁺ T cells were suspended at 5×10^6 cells ml⁻¹ in RPMI 1640 medium containing 1% FBS and 25 mM HEPES. One

hundred microliters of cell suspension was loaded onto the upper wells and placed in a 24-well plate containing 600 μ l of media with the indicated doses of CXCL12 (SDF-1 α) (PeproTech) or CCL19 (ELC) (R&D Systems, Minneapolis, MN, USA). Cells were incubated at 37°C for 90 min, and cells in the bottom wells were counted using a FACSCalibur.

Activation-induced cell death assay

Sorted CD4⁺ GFP⁺ T cells were cultured at a concentration of 1×10^6 cells ml⁻¹ in 96-well plates immobilized with 5 μ g ml⁻¹ of anti-CD3 ϵ mAb (2C11) (BioLegend, San Diego, CA, USA) in RPMI medium supplemented with 10% FBS. Cells were harvested 2 days later and then re-cultured for 3 days in 96-well plates containing immobilized with anti-CD3 mAb or medium containing 200 U ml⁻¹ of human IL-2 (PeproTech). To detect apoptotic cells, a terminal deoxynucleotidyl transferase-mediated deoxyuridine triphosphate nick end labeling assay was performed using the ApopTag Red In Situ Apoptosis Detection Kit (CHEMICON International Inc., Temecula, CA, USA). Briefly, the cells were collected and deposited on glass slides by cytospin (Shandon, London, UK), fixed with PBS containing 1% PFA for 10 min and the DNA free 3' OH were enzymatically labeled with digoxigenin-labeled nucleotides, which were detected using rhodamine-labeled anti-digoxigenin polyclonal antibodies according to the manufacturer's instructions. After applying 6 μ g ml⁻¹ of Hoechst33342 (Invitrogen) for nuclear staining, slides were processed for analysis using an LSM 510 laser-scanning confocal microscope (Carl Zeiss, Jena, Germany). The proportion of apoptotic cells was determined by counting at least 100 cells in the captured images.

T-cell migration in vivo

BALB/c mice were intravenously injected with 2×10^6 of purified CD4⁺ GFP⁺ T cells uninfected or infected with a recombinant adenovirus vector. Twenty-four hours later, the recipient mice were subcutaneously immunized with 0.2 mg of LPS-free OVA in CFA on the back at three sites. The number of CD4⁺KJ1-26⁺ T cells in the draining lymph nodes was measured by flow cytometry at 5 days after immunization.

Adoptive cell transfer

Transfer of B cells and OVA-specific/CD4⁺ T cells infected with a recombinant adenovirus vector in adoptive hosts was performed as described previously (14).

Briefly, CD4⁺ GFP⁺ T cells were prepared by FACS sorting from dTg T cells infected with a recombinant adenovirus vector *in vitro*. B cells were negatively selected from the pooled spleens of either naive mice or 4-hydroxyl-3-nitrophenylacetyl-conjugated chicken γ -globulin (NP-CGG)-primed mice using a MACS system and biotinylated anti-CD5 (53-7.3), anti-CD90.2 (53-2.1), anti-Gr1, anti-CD11b (eBioscience), anti-CD43 (57) and anti-CD138 (281-2) (BD PharMingen). The procedure consistently yielded >95% B220⁺ cells. Purified B cells (5×10^6) together with CD4⁺ GFP⁺ T cells infected with recombinant adenovirus vector (3×10^4) were intravenously injected into CB17-scid mice. One day later, the recipient mice were intraperitoneally challenged with 25 μ g of soluble NP-OVA, and the sera were collected from individual

mice at day 7 after challenge. Anti-NP serum antibody titers were estimated by ELISA assays using NP₂-BSA and NP₁₈-BSA as coating antigens as described previously (14). The relative affinity of anti-NP antibodies was estimated by calculating the ratio of anti-NP₂/anti-NP₁₈ antibody.

Statistics

The results were evaluated statistically by two-tailed Student's *t*-test ($n = 3$) or Mann-Whitney nonparametric test ($n > 4$), with $P < 0.05$ regarded as significant.

Results

Nef impairs T-cell proliferation upon antigen stimulation in vitro

In order to determine the effect of Nef expression in peripheral T cells, we crossed Tg mice that express an OVA-specific T-cell receptor (12) with mice expressing CAR on T cells (11). OVA-specific/CD4⁺/CAR⁺ T cells were purified from the pooled spleens of dTg mice and infected *in vitro* with an adenovirus vector encoding green fluorescence protein (GFP) driven by the CAG promoter with (Ad-nef) or its mutants [Ad-nef (μ)] or without the *nef* gene (Ad) in the presence of IL-7, which supports T-cell survival and promotes progression into the G_{1b} stage of the cell cycle (16, 17). Thereafter, GFP⁺ cells were purified by FACS and provided for analysis as below.

Consistent with previous observations in human T-cell lines, Fig. 1(A) shows that CD4 expression on murine peripheral T cells was down-regulated by Nef but not by the Nef mutant carrying amino acids replacements of ⁵⁷W⁵⁸L to ⁵⁷A⁵⁸A, abrogating the ability to down-regulate CD4 (18). Nef expression had no effect on the expression of CD25, CD28, CD44, CD62L, CD69, TCR β and MHC class I (data not shown).

To examine the effect of Nef in T-cell response, GFP⁺ cells were purified by FACS from CD4⁺/CAR⁺ T cells infected with Ad-nef, Ad-nef (μ) and cultured in the presence of irradiated splenocytes as APCs, which had been pulsed with OVA peptide (OVA₃₂₃₋₃₃₉). Expression of wild-type as well as mutant forms of Nef diminished T-cell proliferation upon stimulations with OVA peptide at a dose of 0.1 μ M (Fig. 1B). These Nef proteins also reduced the level of cytokines produced by T cells in response to different doses of OVA peptide (Fig. 1C). These results suggest that Nef prominently affects T-cell proliferation, irrespective of Nef's ability to down-modulate CD4 but not completely abrogate T-cell activation.

Nef-expression diminishes T-cell migration activity in the primary immune response

Chemokines and their receptors play pivotal roles in the initial homing of lymphocytes and their subsequent trafficking during an immune response (6). It has been reported that Nef impairs the migratory capacity of human T-cell lines *in vitro* in response to the chemokine CXCL12, which binds to T-cell receptor, CXCR4, owing to alteration of the signal cascades downstream of chemokine receptors (7, 15). Consistently, the expression of Nef or its mutant in murine CD4⁺ T cells reduced their migration in response to CXCL12 *in vitro*, without altering the surface receptor expressions (Fig. 2A and B).

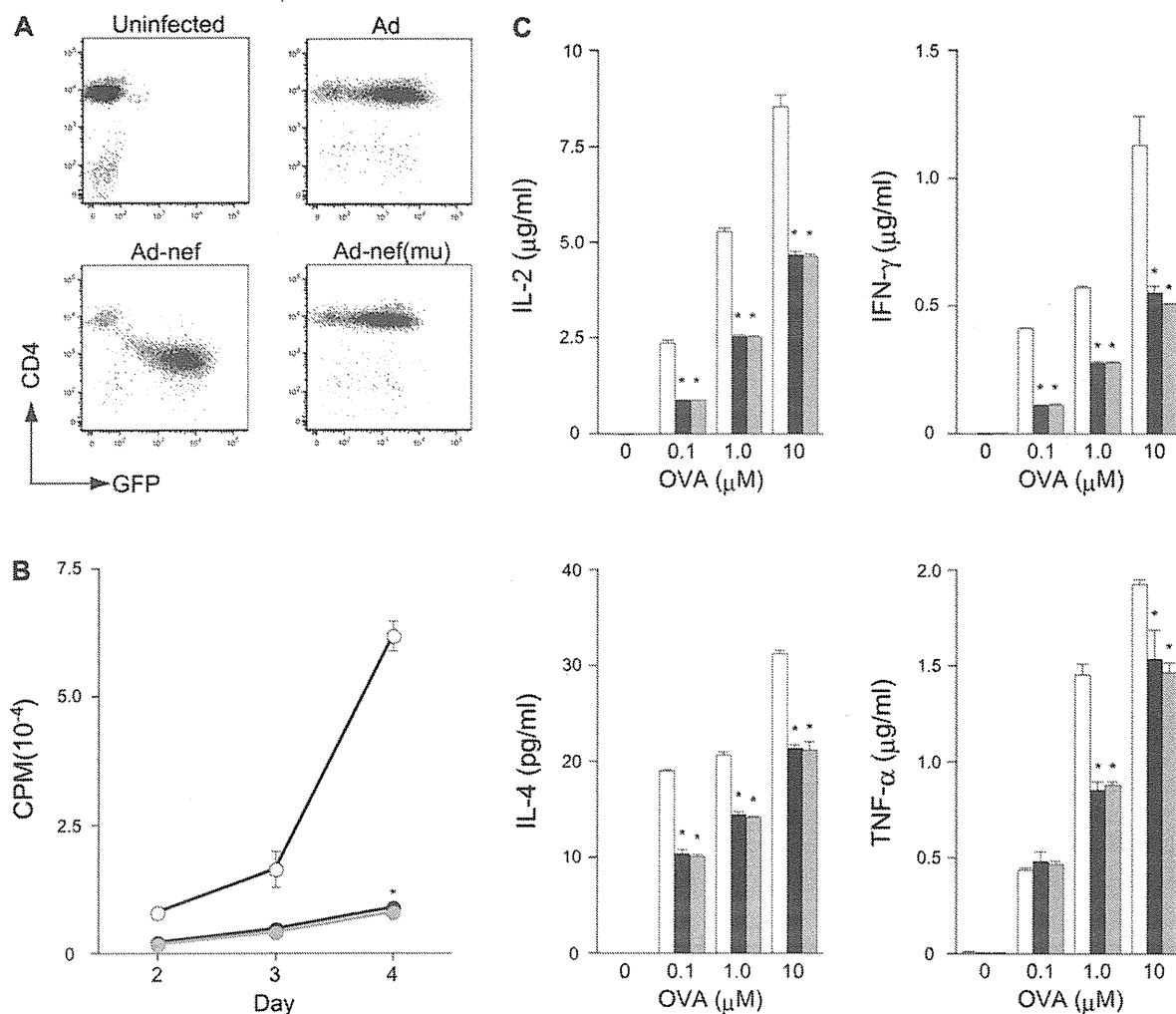


Fig. 1. (A) Characterization of Nef-expressing T cells. A *EGFP* gene-containing adenoviral vector was used to evaluate the efficiency of adenovirus (Ad) infection in DO11.10/*CAR*⁺/*CD4*⁺ T cells. Naive *CD4*⁺ T cells from dTg mice were infected with Ad-nef, Ad-nef (mu) or Ad vector as a control. Two days later, GFP and *CD4* expression were assessed by FACS. (B) Nef represses antigen-specific T-cell proliferation. Purified *CD4*⁺/*GFP*⁺ T cells (5×10^4) infected with Ad-nef (closed), Ad-nef (mu) (gray) and Ad (open) were cultured with T-cell depleted spleen cells as APCs (5×10^5) pulsed with 0.1 μ M of OVA₃₂₃₋₃₃₉ peptide. Their DNA synthesis in the triplicate culture was estimated at the indicated periods by the incorporation of [³H] thymidine added 12 h prior to cell harvest. * $P < 0.001$ versus Ad. (C) Purified *CD4*⁺ *GFP*⁺ T cells and APCs were co-cultured with various concentrations of OVA₃₂₃₋₃₃₉ peptide. Cytokine production in culture supernatant was measured by ELISA on day 3 of culture. * $P < 0.001$ versus Ad. Shown is the representative data from two independent experiments.

Likewise, the Nef proteins, including NL4-3 Nef, did not alter the expression of CXCR4 on human T cells (15, 19), however, there are controversial reports that HIV-1 Nef caused a modest decrease in expression of CXCR4 on human T cells, irrespective of Nef alleles, including NA7 and NL4-3 (7, 20). Further analysis is needed to resolve the discrepancy among these studies.

To examine whether Nef affects T-cell migration *in vivo*, OVA-specific *CD4*⁺ T cells were purified from pooled splenocytes of dTg mice and infected with Ad-nef, Ad-nef(mu) or Ad. These cells were transferred into syngeneic recipients, followed by subcutaneous inoculation with OVA in CFA. Five days later, the frequency of OVA-specific (KJ1-26⁺) *CD4*⁺ T cells in the draining lymph node was estimated by FACS. As shown in Fig. 2(C), we observed that Nef impairs the physiological recruitment of T cells into the secondary

lymphoid tissues in the immune response. A substantial number of *GFP*⁺/*OVA*-specific/*CD4*⁺ T cells infected with Ad accumulated in the draining lymph node after OVA stimulation, however, the number of cells was significantly reduced when the T cells expressed Nef or its mutant. T cells in the draining lymph nodes uniformly expressed high levels of *CD44*, a marker for activated T cells (21), irrespective of their expression of Nef or Nef mutant (Fig. 2D), suggesting that they were activated, but not involved in functional maturation. These results suggest that Nef affects trafficking of T cells to the regional lymph nodes during an immune response, independently of *CD4* down-modulation.

As shown in Fig. 2(E), we examined the possibility that nef expression causes T cells to undergo AICD, which could reduce the number of cells migrating to the regional lymph nodes after stimulation. OVA-specific/*CD4*⁺ or

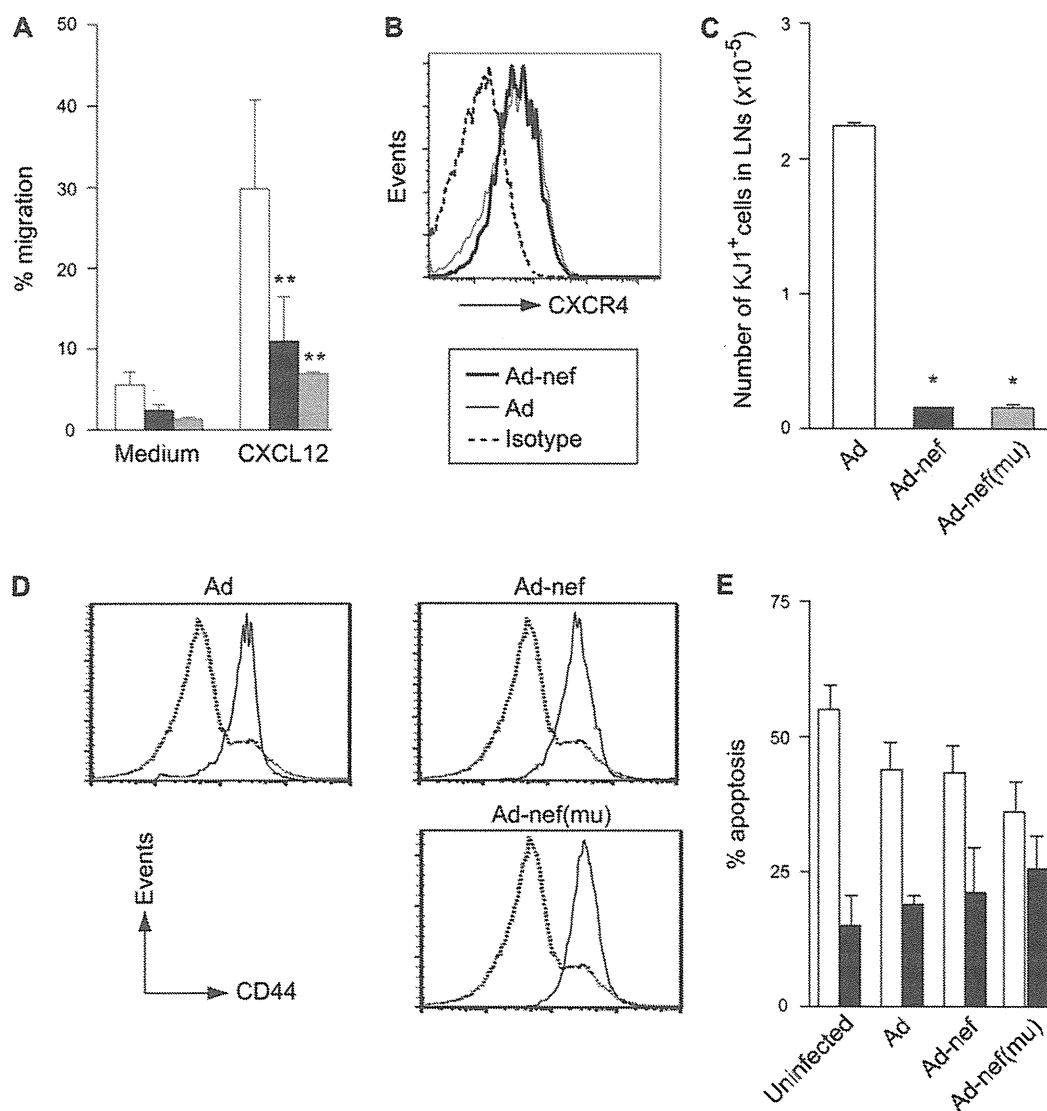


Fig. 2. Nef impairs T-cell migratory activity (A). CD4⁺ GFP⁺ T cells infected with Ad-nef (closed column), Ad-nef (mu) (gray column) and Ad (open column) were used in transwell chemotaxis assays in the presence of CXCL12 (PeproTech). Cells were allowed to migrate in the bottom wells for 90 min, and the proportion of cells that had migrated into the lower wells was determined by flow cytometry. The results are shown as mean \pm SD ($n = 3$). * $P < 0.01$ versus Ad. (B) CXCR4 surface staining for CD4⁺/GFP⁺ T cells after infection with Ad-nef (solid line) or Ad (thin line), together with control IgG staining (broken lines). (C and D) CD4⁺/GFP⁺ T cells (2×10^6) infected with Ad-nef (closed column), Ad-nef (mu) (gray column) and Ad (open column) were transferred into BALB/c mice and 24 h later mice were injected subcutaneously with 0.2 mg of LPS-free OVA with CFA on the back in three sites. The cell number (\pm SD) of CD4⁺/OVA-specific T cells in the draining lymph nodes (C) and the level of CD44 expression in Ad-infected donor (solid line) and recipient CD4⁺ T cells (broken line) (D) were measured by flow cytometry using anti-CD4, anti-CD44 and KJ1-26 mAbs on day 5 after OVA injection. * $P < 0.001$ versus Ad. (E) CD4⁺ T cells (1×10^6) or CD4⁺/GFP⁺ T cells (1×10^6) infected with Ad-nef, Ad-nef (mu) and Ad were stimulated with immobilized anti-CD3 ϵ mAb for 2 days, followed by re-stimulation with anti-CD3 mAb/IL-2 (open column) or IL-2 alone (closed column) for 3 days. Apoptotic cells were analyzed by terminal deoxynucleotidyl transferase-mediated deoxyuridine triphosphate nick end labeling assay. Representative data from two independent experiments in (A), (C) and (D) and from three independent experiments (B) is shown.

OVA-specific/CD4⁺/GFP⁺ T cells were hyperstimulated with immobilized anti-CD3 ϵ mAb at 2-day intervals as previously described (22). The results show that Nef did not enhance the induction of AICD in T cells upon TCR-stimulation *in vitro* nor did it compromise the survival function mediated by IL-2. Therefore, it seems unlikely that Nef causes T-cell death, which could reduce the number of cells migrating to the regional lymph nodes.

Nef expression in T cells affects the primary and memory B-cell responses

To examine T-cell helper activity by Nef, OVA-specific/CD4⁺ T cells were purified from the pooled spleens of dTg mice, followed by infection with or without Ad-nef, Ad-Nef (mu) or Ad. The GFP⁺/CD4⁺ T cells were purified by FACS (Fig. 3A) and transferred into CB17-scid mice, together with either naive or NP-primed B cells. The recipients were immunized

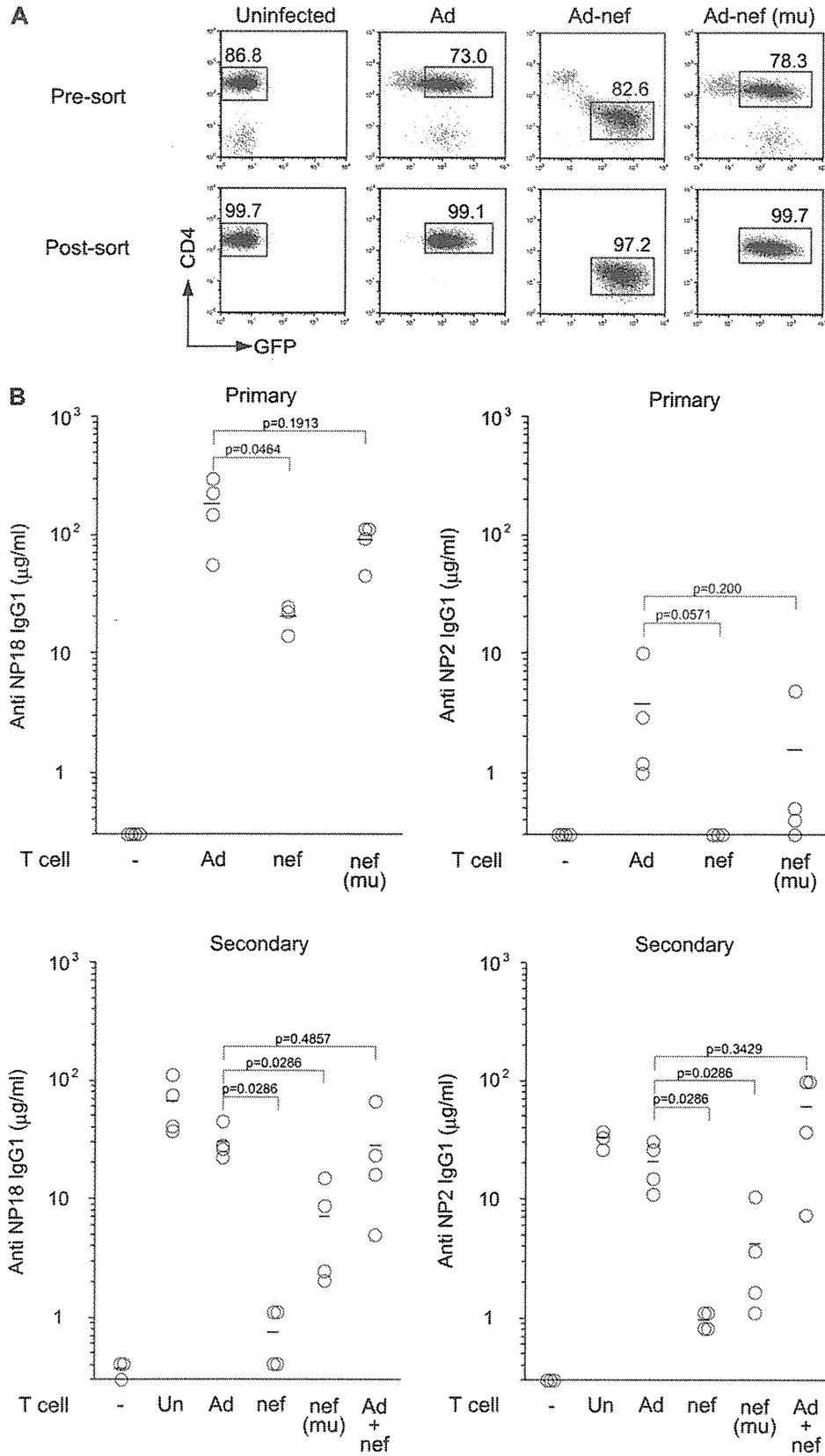


Fig. 3. Nef affects primary and memory B-cell response. (A) OVA-specific/CD4⁺ T cells were purified from dTg mice and infected with Ad-nef, Ad-nef (mu) and Ad, followed by FACS purification (Post-sort). Numbers in plots indicate percent of GFP⁻ uninfected cells and GFP⁺ cells before (Pre-sort) and after purification (Post-sort). (B) Purified GFP⁺ T cells (3×10^4) were transferred into CB17-scid mice, together with

with NP-OVA in alum for the primary response or soluble NP-OVA for the secondary response (Fig. 3B).

The results show that Nef expression in T cells reduced the level of anti-NP IgG1 serum antibodies by ~10-fold (NP₁₈; $P = 0.0464$, NP₂; $P = 0.0571$) in the primary response (Fig. 3B), whereas when the T cells were infected with Ad-Nef (μ), which does not down-regulate CD4 (Fig. 3A), the response was close to the control level (NP₁₈; $P = 0.1913$, NP₂; $P = 0.200$). As shown in Fig. 3(B), the impact of Nef on the secondary response was even more dramatic; there was a 30- to 40-fold reduction in both total and high-affinity anti-NP IgG1 antibodies (NP₁₈; $P = 0.0286$, NP₂; $P = 0.0286$). Reconstitution with equal numbers of non-infected and Nef-expressing OVA-specific CD4⁺ T cells normalized the secondary adoptive response (NP₁₈; $P = 0.4857$, NP₂; $P = 0.3429$), excluding the possibility that Nef expression was generating suppressor T cells. Expression of the Nef mutant that was unable to down-modulate CD4 also reduced the secondary response (NP₁₈; $P = 0.0286$, NP₂; $P = 0.0286$), although the magnitude of the reduction was less than that induced by expression of wild-type Nef. These results demonstrate that Nef expression in peripheral T cells markedly diminishes their helper activity for the secondary IgG1 response and that this defect was only partially associated with the Nef-induced CD4 down-modulation. By contrast, this CD4 down-regulation appeared to be even more important for the reduced primary IgG1 response. These findings underscore the differential regulation in the primary and memory B-cell response. Thus, Nef affects helper T-cell activities in the primary and secondary response through different processes with different CD4 down-modulation susceptibility.

Discussion

In the present study, we have examined the consequence of Nef expression in primary splenic T cells. In order to avoid complications arising from expression of Nef early in T-cell development, e.g. lymphopenia, we established a double transgenic mouse (dTg), which expresses human CAR adenovirus receptor and an OVA-specific T-cell receptor that recognizes the OVA peptide on APC with high affinity under MHC Class II I-A^d-restriction. OVA-specific/CD4⁺ T cells were purified from the spleen of dTg mice and infected with a recombinant adenovirus vector encoding Nef and GFP, followed by purification of GFP⁺ cells using flow cytometry. To promote efficient introduction of the adenovirus vector into resting T cells, they were cultured for 2 days in the presence of the vector and IL-7, which is known to be important for survival of naive and memory T-cell populations (16). Neither naive nor memory CD4⁺ T cells proliferate in response to IL-7, but they progress into the G_{1b} stage of the cell cycle (17). Thus, the present system allowed us to study the role

of Nef in resting T cells in response to antigen-specific stimulation *in vitro* and *in vivo*.

During HIV-1 infection, the virus enters resting CD4⁺ T cells and Nef is expressed even before the virus is integrated (1). It has been previously suggested that Nef expression in resting human T cells enhances IL-2 production upon activation by TCR cross-linking (1). This led to the proposal that Nef may enhance TCR signaling pathways that could help virus replication in partially stimulated T cells. In line with this viewpoint, it has been reported that Nef in human leukemic T cell lines and CD4⁺ T-cell lines established from PBMC enhanced TCR signaling pathways and activated IL-2 production upon stimulation with TCR/CD28 or mitogens (2–5). In addition, Nef affects activation of murine T-cell hybridomas stimulated with anti-CD3 mAb (23), suggesting that the effect of Nef is not species specific.

In striking contrast, the present study demonstrates that Nef significantly reduces OVA-specific T-cell activation *in vitro* as defined by reduced proliferation and cytokine production, including IL-2 and IFN γ , but not completely. Furthermore, we demonstrate for the first time that Nef expression in OVA-specific resting T cells in the periphery reduced their ability to help anti-NP/IgG1⁺ primary and secondary antibody responses in adoptive hosts after immunization with NP-OVA. In addition, in agreement with a previous *in vitro* analysis (7, 15), our *in vivo* results support the notion that Nef impairs the physiological recruitment of lymphocytes from the blood into the secondary lymphoid tissues after primary immunization, which promotes efficient antigen presentation and immune responses. Thus, Nef expressed in T cells at the early cell cycle stage impairs multiple functions in their subsequent antigen-specific response *in vivo*.

Why is the Nef-associated T-cell hyperresponse previously reported not detected in the present studies? The discrepancy does not reflect the differences in pathogenesis in Nef alleles (24) because the previous transgenic mouse models (8–10) and the present studies used the same NL4-3 Nef for characterization of the role of Nef protein in the immune system. Furthermore, the activation phenotype of T cells *in vitro* was induced by Nef proteins, irrespective of their alleles, including NL4-3 Nef (2–5). The discrepancy could be due to the cell state in the previous studies caused by transient over-expression of the protein in either the Jurkat T-cell line or in an activated human CD4⁺ T-cell line established from PBMC (2–7). Another possible explanation is that previously reported assays utilized different TCR stimuli; the cells were stimulated by strong TCR ligation using immobilized antibodies (2–5). Such strong TCR ligation by antibodies forms stable TCR aggregates associated with the signaling complex (25). However, TCR stimulation with APC-presented antigen peptide forms an immunological synapse (IS) at the

B cells (5×10^6) which were enriched from the pooled spleens of either naive or 4-hydroxyl-3-nitrophenylacetyl-conjugated chicken γ -globulin (NP-CGG)-primed mice using a MACS system, followed by challenge with 100 μ g of NP-OVA in alum (primary) or 25 μ g of soluble NP-OVA (secondary). Serum anti-NP antibody titers were estimated by ELISA assays at day 7 after challenge using NP₂-BSA and NP₁₈-BSA as coating antigens. The relative affinity of anti-NP antibodies was estimated by calculating the ratio of anti-NP₂/anti-NP₁₈ antibody. Representative data from two independent experiments is shown. Bars represent the mean of each group.